sustainability

MDPI

Article

A New Efficient Cuckoo Search MPPT Algorithm Based on a Super-Twisting Sliding Mode Controller for Partially Shaded Standalone Photovoltaic System

Zahra Bel Hadj Salah [1,*], Saber Krim [2,3], Mohamed Ali Hajjaji [1,4], Badr M. Alshammari [5], Khalid Alqunun [5], Ahmed Alzamil [5] and Tawfik Guesmi [5]

[1] Electronic and Micro-Electronic Laboratory, LR99ES30, Faculty of Sciences, University of Monastir, Monastir 5000, Tunisia; mohamedali.hajjaji@issatso.rnu.tn
[2] Laboratory of Automatic, Electrical Systems and Environment, National Engineering School of Monastir, University of Monastir, Monastir 5000, Tunisia; krim.saber.enim@gmail.com
[3] Department of Technology, Higher Institute of Applied Sciences and Technology of Kasserine, University of Kairouan, Kairouan 3100, Tunisia
[4] Higher Institute of Applied Sciences and Technology, University of Sousse, Sousse 4003, Tunisia
[5] Department of Electrical Engineering, College of Engineering, University of Ha'il, Ha'il 2240, Saudi Arabia; bms.alshammari@uoh.edu.sa (B.M.A.); kh.alqunun@uoh.edu.sa (K.A.); aa.alzamil@uoh.edu.sa (A.A.); tawfik.guesmi@istmt.rnu.tn (T.G.)
* Correspondence: zahra.hadjsalah@gmail.com

Abstract: The impact of Partial Shading Conditions (PSCs) significantly influences the output of Photovoltaic Systems (PVSs). Under PSCs, the Power-Voltage (P-V) characteristic of the PVS unveils numerous power peaks, inclusive of local maxima and a global maximum. The latter represents the optimum power point. Traditional Maximum Power Point Tracking (MPPT) algorithms struggle to track the Global Maximum Power Point (GMPP). To address this, our study emphasizes the creation of a novel algorithm capable of identifying the GMPP. This approach combines the Cuckoo Search (CS) MPPT algorithm with an Integral Super-Twisting Sliding Mode Controller (STSMC) using their benefits to enhance the PVS performance under PSCs in terms of high efficiency, low power losses, and high-speed convergence towards the GMPP. The STSMC is a second-order Sliding Mode Control strategy that employs a continuous control action that attenuates the "chattering" phenomenon, caused when the first-order SMC technique is employed. Indeed, the proposed CS-STSMC-MPPT algorithm consists of two parts. The first one is based on the CS algorithm used for scanning the power-voltage curve to identify the GMPP, and subsequently generating the associated optimal voltage reference. The second part aims to track the voltage reference by manipulating the duty cycle of the boost converter. The proposed CS-STSMC-MPPT algorithm is featured by its strength against uncertainties and modeling errors. The obtained simulation results underline a high convergence speed and an excellent precision of the proposed method in identifying and tracking the GMPP with high efficiency under varying shading scenarios. For comparative purposes, this method is set against the hybrid CS-Proportional Integral Derivative, the conventional CS, the Particle Swarm Optimization, and the Perturb and Observe algorithms under different PSCs, including zero, weak, and severe shading. Simulation conducted in the Matlab/Simulink environment confirms the superior performance of the proposed CS-STSMC-MPPT algorithm in terms of precision, convergence speed, efficiency, and resilience.

Keywords: photovoltaic system; partial shading conditions; maximum power point tracking; cuckoo search algorithm; second-order super-twisting sliding mode control

check for updates

Citation: Hadj Salah, Z.B.; Krim, S.; Hajjaji, M.A.; Alshammari, B.M.; Alqunun, K.; Alzamil, A.; Guesmi, T. A New Efficient Cuckoo Search MPPT Algorithm Based on a Super-Twisting Sliding Mode Controller for Partially Shaded Standalone Photovoltaic System. *Sustainability* **2023**, *15*, 9753. https://doi.org/10.3390/su15129753

Academic Editors: Ali Kecebas and Emine Yağız Gürbüz

Received: 15 April 2023
Revised: 10 June 2023
Accepted: 13 June 2023
Published: 19 June 2023

Copyright: © 2023 by the authors. Licensee MDPI, Basel, Switzerland. This article is an open access article distributed under the terms and conditions of the Creative Commons Attribution (CC BY) license (https://creativecommons.org/licenses/by/4.0/).

1. Introduction

The increasing energy demand worldwide has given rise to a viable solution which is solar energy thanks to its purity, limitlessness, and eco-friendliness [1,2]. Nevertheless, seasonal variations and weather conditions have an impact on the electricity supplied by Photovoltaic Systems (PVSs), especially solar radiation and environmental temperature variation. These conditions along with the nonlinear relationship of the PVS output current and voltage can reduce the energy conversion efficiency of the Photovoltaic (PV) panels and can result in the non-similarity of the Maximum Power Point (MPP) and the PV panel operating point. Therefore, MPP Tracking (MPPT) is necessary to find and extract the MPP at its ideal value [3,4].

Usually, the curve of the P-V characteristic has one peak due to the nonlinearity of the PV output characteristics, under even irradiation [5]. However, the PVS may still come into contact with a variety of environmental elements, including clouds, dust, leaves, buildings, bird droppings, electric poles, and others. These can readily throw uneven shadows on the surface of the PV array, which can cause multiple peaks on the P-V output [6,7] where the maximum amount of power produced is defined as a Global MPP (GMPP) [8] presented by the biggest peak, and the others represent the Local MPP (LMPP). Then, reliable GMPP Tracking (GMPPT) is necessary under Partial Shading Conditions (PSCs).

The efficacy of these MPPT controllers lies in their ability to provide accuracy, robustness, and high tracking speed. To this end, various MPPT techniques have been proposed, all designed to enhance the PVS performance. These techniques can be classified into several categories, and each class has its strengths and weaknesses. The most known is the conventional algorithm thanks to its simplicity and satisfactory performance, under particular conditions, such as Perturb and Observe (P&O) [9,10] and Incremental Conductance (INC) [11]. Simplicity, low implementation costs, and satisfactory performance are the benefits of conventional techniques. However, they have several limitations, including the steady-state accuracy of the PV output power around the MPP [12], the slow tracking speed under a rapid variation in solar irradiance and the inefficiency of GMPPT under PSCs [13]. They often fail to distinguish the GMPP from LMPPs, typically resulting in these methods being trapped at the LMPP. Consequently, this leads to a substantial loss in the overall power output of the PVS. These flaws can drastically reduce the PVS performance.

These shortcomings underline the need for advanced MPPT techniques, capable of identifying the GMPP even under PSCs. Hence, to distinguish the real GMPP from other LMPPs, a variety of MPPT methodologies and alternate solutions have been employed in the literature [14–16]. In Ref. [17], the authors discussed the challenges that PSCs posed to the efficiency of PV power generation and the MPPT. To address these issues, the authors suggested the use of an Artificial Neural Network (ANN) model to predict the MPP under PSCs. The authors in [18] outlined an examination of 20 optimized GMPPT methods, all tested under the same platform involving a PV boost feeding a battery. The shading patterns and sampling time were standardized to maintain consistency across all tests. The focus of the review [19] was centered on several crucial GMPPT strategies. These strategies included the improved conventional methods which were recognized for their significance in enhancing the efficiency of PVs under varying conditions. Further details of these algorithms and their respective performance evaluations were provided to better understand their applicability and potential. The authors in [20] offered a comprehensive review of various MPPT techniques, focusing on their classifications as offline, online, and hybrid techniques. These were assessed under both uniform and non-uniform irradiance conditions. The authors in [19] highlighted that intelligent MPPT techniques outperformed both offline and online methods in terms of tracking accuracy, efficiency, and minimized steady-state oscillations. Furthermore, intelligent techniques tracked the GMPP under PSCs and the effect of the PSC on MPPT remained a key issue for researchers to resolve.

Building on the comprehensive review in the aforementioned articles, it is clear that intelligent methods such as Artificial Intelligence (AI) methodologies have demonstrated a notable capability of handling the complexities and irregularities of such conditions, effectively optimizing the PVS performance. AI-based techniques such as Fuzzy Logic Control (FLC) [13] and ANN [21–26] have emerged as robust tools in addressing the challenges presented by varying irradiance conditions, particularly under partial shading. These methods excel in dealing with non-linear and uncertain systems, often resulting in enhanced efficiency and reliability of power tracking in PVS under different conditions. These algorithms can manage the multiple power peaks induced by PSCs, efficiently tracking the GMPP. They have been demonstrated to improve the accuracy, efficiency, and reliability of MPPT enhancing the overall performance of PVSs. However, it is worth noting that these methods come also with challenges. They can be computationally intensive, requiring significant processing power and often more complex hardware. The need for large amounts of training data can be a limitation as well, especially in contexts where data may be difficult to collect [21–26]. These challenges highlight the need for alternate strategies that can address the shortcomings of AI, particularly in the context of PVSs and GMPPT. Metaheuristic algorithms offer a compelling solution in this regard. These techniques, such as Particle Swarm Optimization (PSO) [27,28], Genetic Algorithms (GAs) [29,30], Simulated Annealing (SA) [31], and Ant Colony Optimization (ACO) [32], Grey wolf optimization (GWO) [33], Crew Search Algorithm (CSA) [15], and Cuckoo Search (CS) algorithm [16], and others, have shown to be highly effective in GMPPT under PSCs. These algorithms offer flexibility and are capable of exploring a broad solution space to find near-optimal solutions in a reasonable time frame. In light of the strengths of these techniques, and considering their suitability to handle the complex GMPPT optimization problem under PSCs, our work is based on the application of metaheuristic algorithms. Given their potential to improve the efficiency and reliability of PVSs under PSCs, this direction of research is compelling and warrants further exploration [34]. Metaheuristics, with their demonstrated advantages [35], appear well-suited to address the challenges posed by GPPT in PVSs under PSCs. However, it is equally important to acknowledge that these methods come with their own set of challenges, such as the potential for premature convergence and the need for careful parameter tuning.

Among the most important meta-heuristic methods, the PSO-MPPT algorithm was introduced by James Kennedy and Russel Ebhart in 1995 [36]. PSO-MPPT algorithm is a swarm intelligence-based metaheuristic approach inspired by the intelligent social movement of birds in flocks. This method is an efficient method in tracking the MPP even under PSCs, but it takes a long time convergence [36,37]. PSO-MPPT is sensitive to the parameters of the algorithm since it uses three parameters: ω, c1, and c2 corresponding to the inertia weight, cognitive, and social coefficients, respectively. Bad selection of these parameters can lead to blocking in the local optimum or a slow convergence [38]. Generally, the CS-MPPT algorithm is less sensitive to the parameters and can better avoid the local optimum thanks to the levy random walk which makes it more robust in different situations [16,38–44]. Therefore, our work is based on this algorithm.

The CS-MPPT algorithm is a highly popular metaheuristic method [40,44] renowned for its fast convergence time and minimal steady-state error [45]. Researchers from diverse fields have taken great interest in the CS algorithm and successfully applied it to solve a range of problems [46]. Simplicity, few control parameters, and ease of implementation, along with its quick convergence and low steady-state error, contribute to its widespread adoption. However, a notable limitation of the conventional CS algorithm lies in its random initialization of cuckoo populations within host nests. This limits its global exploration ability, affects the convergence performance, and increases the probability of becoming trapped in a local optimum in multi-optima systems [47].

Numerous solutions have been suggested to improve the effectiveness of the conventional CS algorithm when applied to the GMPP under PSCs. In Ref. [48], the author introduced an improved CS algorithm for MPPT in PV module arrays. The algorithm enhanced tracking efficiency by adjusting the step factor based on the PV characteristic curve slope and a number of iterations. The simulation results show that the improved algorithm achieved faster and more precise MPPT, improving power generation efficiency under various shading conditions. It demonstrated robustness and adaptability, applicable to different connection configurations without any parameter modification. In Ref. [49], the authors focused on enhancing the conventional CS algorithm through the introduction of a novel approach known as Dynamic CS (DCS). In contrast to the conventional algorithm, which employed a small set of randomly generated initial values, the DCS method adopted a different strategy by generating a larger number of initial particles with incrementally increasing values. Additionally, the study proposed an optimized algorithm that restricted the search space based on the evolution of duty cycle values and the discrepancy between the maximum and minimum values of PV output powers. This optimization technique enabled efficient swapping of the entire particles' search space, leading to a prompt and seamless convergence towards the steady GMPP. The method that was developed demonstrated exceptional precision and reliability in achieving MPPT in PV arrays. It exhibited high tracking speed and effectively minimized output power fluctuations, enhancing the overall performance of the PVS. In Ref. [43], an enhanced CS algorithm was presented. This improved algorithm addressed the limitations of the conventional approach. By reducing the exploration area after each iteration, the proposed algorithm improved the convergence time, minimized the power oscillation, and reduced the system power losses. The simulation and practical experiments showed that the suggested algorithm outperformed other methods, demonstrating its effectiveness in optimizing the search process for MPPT. The algorithm named in [16] as the Improved CS (ICS), enhances the tracking mechanism of the Original CS (OCS) algorithm. The ICS algorithm employed a novel strategy where the worst particle was attracted toward the global best. This was achieved by adjusting the position of the worst cuckoo using the difference between the worst and best cuckoo positions, multiplied by a random value. By iteratively replacing the worst cuckoo with a particle closer to the best cuckoo, the algorithm achieved faster convergence and improved steady-state performance. The article presented simulation and experimental results, demonstrating the effectiveness of the ICS algorithm in reducing convergence time and steady-state oscillations. These findings highlighted the superiority of the ICS algorithm over the original CS strategy and other optimization techniques considered in the study. Moreover, the authors recommended using four searching agents with the ICS algorithm when dealing with P-V curves that have more than five peaks. However, if the number of peaks exceeds five, they suggest using six agents for optimal performance. Increasing the number of agents in an optimization algorithm could impact the complexity of the system. As the number of agents increased, the computational and memory requirements of the algorithm typically would rise, resulting in higher complexity. Similarly, the utilization of three parameters in the ICS-MPPT algorithm contributed to its overall complexity.

In order to enhance the performance of the CS-MPPT algorithm, a Proportional-Integral-Derivative (PID) controller was integrated with the CS, resulting in a hybrid CS-PID approach, as shown in [42]. The integration of these two techniques aimed to mitigate the challenges posed by PSCs in PVSs. This hybrid method aimed to effectively track GMPP while simultaneously reducing the tracking time and eliminating the fluctuations around the GMPP. The CS component of the hybrid approach was responsible for providing the maximum voltage required for efficient power point tracking. The voltage supplied by the CS was compared with the reference voltage. The difference between these voltages, known as the error voltage (e), was then input into the PID controller. The PID controller processed the error voltage and generated a control signal. This control signal was subsequently used to trigger the switching device of the converter, ensuring that the converter produced the desired output voltage. The PID controller parameters were K_p, K_i, and K_d, which were the proportional, integral, and derivate coefficients, respectively. Any variations in these coefficients or external disturbances could impact the robustness and performance of the PVS. Proper tuning of the PID controller parameters is essential to ensure optimal performance and stability in the presence of variations or disturbances [50–52]

To avoid the pitfalls of improperly tuning the PID controller and its impact on the system performance, researchers have proposed numerous sophisticated non-linear control strategies for MPPT [53,54]. These included adaptive control [27], predictive control [28], backstepping-based control [55], and intelligent control methods rooted in ANNs and fuzzy logic systems, as well as sliding mode control (SMC) [53,54,56,57].

SMC stands out among nonlinear control techniques for its robustness, fast response, and easy implementation. Notably, it effectively operates without exact system parameters. Due to these benefits, it has been widely used in various research and industrial applications [58]. However, the limit of the First Order SMC (FOSMC) solution in the existing literature is a chattering problem [59]. This phenomenon generates undesirable fluctuations in the output power and reduces the efficiency of energy harvesting. In order to mitigate this issue, many studies have been designed to improve SMC performance. The enhancement involves introducing an integral term to the sliding surface, thereby creating what is known as an integral SMC to eradicate the steady-state error and diminish chattering [60]. In addition, chattering can be mitigated by implementing saturation or sigmoid functions as an alternative to discontinuous control actions. This approach ensures a continuous control action, thus reducing chattering. However, it is important to note that this control law directs the system state trajectories not exactly to the sliding surface, but to an area in its proximity. Consequently, this might impact the control robustness in handling disturbances [60,61]. Additionally, AI techniques have emerged as potent solutions to this issue. These methods essentially leverage human understanding of the controlled system operations, hence achieving robust control with minimal errors [62]. In Ref. [63], the authors suggested the use of a fuzzy logic system as a substitute for the saturation function in the reaching control law. This proposed solution could potentially minimize chattering, even in the face of significant disturbances.

Additionally, High-Order SMC (HOSMC) has been endorsed by numerous researchers [64–66] as an optimal solution to circumvent the drawbacks of FOSMC, while preserving its benefits. it has garnered significant attention from researchers [57] due to several compelling characteristics. The SOSMC technique has proven to be successful due to its multiple advantageous properties. Firstly, it effectively reduces chattering. Secondly, it demonstrates robustness against parameter uncertainties and external disturbances, making it highly reliable in a variety of challenging conditions. Finally, it is characterized by high efficiency, ensuring optimal system performance. These attributes make it an excellent solution to overcome the flaws of FOSMC. SOSMC requires information about the sliding surface and its time derivative [67]. The only exception is that Integral Super-Twisting (STSMC) can be chosen. The latter uses SOSMC and needs only the information about the sliding surface [56]. This helps lessen chattering and makes the system work better thanks to its continuous control action. Moreover, STSMC is known for its robustness and has precise tracking with fewer errors. It also responds well to changes and is easy to design and put into action [57,59,68].

Therefore, in our work, we combine CS-MPPT with STSMC to create a robust hybrid controller that excels in tracking performance. Indeed, the proposed controller swiftly and precisely tracks the GMPP, under PSCs. In fact, the CS-MPPT algorithm generates a reference voltage corresponding to GMPP. We choose the SMC for its myriad advantages. Furthermore, our hybrid controller outperforms traditional methods in terms of speed and precision under PSCs. To demonstrate the efficiency and good performance of GMPPT in terms of high efficiency, low convergence speed, and simplicity, the CS-STSMC-MPPT algorithm is tested and compared to the CS-PID, CS, PSO, and P&O MPPT algorithms.

Therefore, the main novelty and contributions of this paper in both theory and simulation studies are as follows:

(i) Introducing a new MPPT technique based on the combination of CS-MPPT with STSMC while benefiting from the advantages of both methods to ensure good performance in terms of high efficiency, high-speed convergence, and robustness.
(ii) Highlighting the good performance of the proposed CS-STSMC-MPPT algorithm in terms of efficiency to extract the maximum power even under PSCs, convergence time, and power losses by comparing it with the CS-PID, CS, P&O, and PSO-MPPT methods. This is new in terms of using such algorithms.
(iii) Highlighting the efficacy of the proposed CS-STSMC-MPPT algorithm to overcome the negative effect of partial shading by comparing its performance under different

scenarios, which are zero, severe, and heavy shading conditions. The novelty here is the combination of the CS, and the STSMC methods.

(iv) Highlighting the importance of the proposed CS-STSMC-MPPT algorithm through qualitative and quantitative comparison with other methods. Again, our contribution resides in combining both methods

The remainder of the paper is structured as follows: first, Section 2 presents a classification of the different MPPTs with an analysis of their strengths and weaknesses. In Section 3, the challenges that can affect the performance of MPPT are noted. The PVS and the boost converter, which compose the power system, are mathematically modeled in Section 3. Then, the simulated MPPT techniques in this work are presented in Section 4. Section 5 illustrates the global system. After that, a comparison between the proposed CS-STSMC, CS-PID, CS, PSO, and P&O MPPT algorithms in terms of efficiency, convergence time, and power losses is explained in Section 6. The conclusion is presented in Section 7.

2. Evaluation of MPPT Methods

In the literature, there has been some research on MPPT algorithms, which have been classified into different categories based on the topics discussed. Each category examines specific aspects of these algorithms. In Refs. [69–74], a lot of classifications were proposed based on different criteria. In our research work, the MPPT algorithms are classified into traditional [73], soft computing [75,76], and hybrid techniques [77]. Conventional methods are direct and indirect. The metaheuristic method, AI, and the chaos theory are categories for soft computing methods [30,31,78], whereas the hybrid MPPT approaches combine two or more novel and/or conventional MPPT algorithms [79].

In general, conventional MPPT methods can be categorized into two main groups based on their approach to tracking the MPP. These techniques are generally simpler and easier to implement but they may be less accurate, especially under varying environmental conditions, and they can fail in tracking the GMPP under PSCs. To overcome the drawbacks of conventional MPPT techniques, researchers have turned towards soft-computing [40,76], which has proved advantageous in tracking the PVS GMPP under PSCs. Soft-computing MPPT methods are subcategorized into chaos theory, AI, and metaheuristics [15,16]. The chaotic search method is a random algorithm that can be employed to locate the optimal solution for dynamic problems. In the case of MPPT problems, the PV voltage is selected as the variable to optimize, and the PV-generated power is the chosen fitness function. The search process begins by defining search points and selecting two low points as the search zone end points. With each iteration, the search zone progressively reduces in size until it reaches the MPP. Due to the non-linear properties exhibited by solar PV modules, AI-based methods are widely regarded as the most effective approach for tackling these types of issues [80,81]. These methods are beneficial for addressing nonlinear problems that arise in real-world scenarios. By eliminating the need for a complete mathematical model of the system, AI methods can deliver effective solutions with only prior knowledge of the system. Metaheuristic methods are widely used to tackle complex problems that were previously difficult to solve. These optimization algorithms, inspired by natural processes and intelligence, offer distinct advantages [82]. They excel in exploring complex search spaces, finding optimal solutions, and handling multimodal optimization problems. Particularly under PSCs, metaheuristic methods prove to be suitable for MPPT by overcoming local optima through global search strategies, demonstrating robustness in handling non-linear and non-convex optimization problems, and adapting to dynamic changes in shading conditions. The application of metaheuristic algorithms results in improved efficiency and accuracy of MPPT, making them a valuable tool in optimizing PVS under PSCs. In Ref. [24], metaheuristic algorithms gained significant popularity because of their benefits. Metaheuristic MPPT methods were classified into swarm intelligence, mathematical, evolutionary, and bio-inspired algorithms. However, the initialization of these algorithms is a critical point. In addition, hybrid methods lie on combining between two algorithms advantageously. However, it is important to note that while hybrid methods offer improved performance, they also introduce additional complexity to the MPPT process [83].

Table 1 summarizes all MPPT algorithm categories and presents the merits and demerits of each one. From Table 1, we note that MPPT is evaluated according to many criteria such as efficiency [84], tracking speed [85], accuracy [86], implementation complexity [87], and good performance in different atmospheric conditions especially shading conditions [88]. Based on these criteria, it can be seen that conventional methods are the simplest and most inefficient in PSCs [89], whereas, AI methods are efficient but their ability to track the GMPP is not guaranteed. On the other hand, metaheuristic methods succeed in extracting the GMPP under PSCs and are sensitive to initial conditions depending on the tuning parameters. As each class of MPPT has its drawbacks and qualities, hybrid methods improve the algorithm efficiency by combining the benefits of each one used. These methods are powerful but complex. Based on this analysis, we have chosen to work on metaheuristic methods, given their effectiveness in the case of PSCs and their simplicity.

Table 1. MPPT algorithms.

MPPT Classes		Examples	Advantages	Disadvantages
Conventioanl methods	*Direct*	• P&O [90], • INC, • Hill Climbing [91]	• Simplicity, • Low implementation cost • Satisfactory performance	• Steady-state accuracy of PV output power around MPP [12] • Slow tracking speed under rapid variation in solar irradiance • Inefficiency of GMPPT under PSCs [13].
	Indirect	• Fractional open circuit voltage [92,93] • Fractional short circuit current [94] • Look up table [95,96]		
Soft-computing methods	*Chaos search method* [21,96–99]	-	• Ability to track MPP • Fast convergence time • Robustness against parameter variations • High efficiency [100]	• Complexity • Parameters must be correctly tuned • Noise sensitivity • High oscillations around MPP specially under PSCs • Initialization dependence
	AI MPPT algorithms [80]	• ANN [101] • FLC [102]	• Computationally efficient, flexible, and rapid response to MPPT challenge [103] • Strong performance even in presence of changing system parameters • No need of exact input to extract MPP • Fast tracking speed in case of fast change of illumination • Slight fluctuation	• Need of a massive dataset [21–26] • Not continual succeed to track the GMPP under PSCs • Requiring a lot of calculations and costly realization.
	Metaheuristic MPPT [82]	• CS algorithms [16] • GA [30] • DE [104] • PSO [27,28], • Ant colony optimization [32] • Modified PSO [105], • S-jaya [106] • Simulated annealing [31] • Teaching-learning-based-optimization [107] • Artificial Bee Colony [108] • Firefly algorithm [109] • Flower Pollination (FPA) [110], • GWA [33]	• GMPPT ability • High efficiency under different weather conditions • Robustness • Flexibility • Lack of gradient requirements • Ability to avoid local optima	• Sensitivity to initial conditions • Sensitivity to tuning parameters

Table 1. *Cont.*

MPPT Classes	Examples	Advantages	Disadvantages
Hybrid methods	• P&O with ANN [33] • GWA with P&O [111] • Firework with P&O [112] • PSO with P&O (PSO-P&O) [113] • Firefly with INC [114] • Bat search with P&O [115].	• High speed convergence • High efficiency	• Cost of hardware implementation, • Sensor requirement • Design complexity level

3. Challenges of MPPT Algorithms

It is challenging to determine whether or not the MPPT algorithm is good because there are numerous issues that can affect its performance. There is a risk that developers fail to account for issues such as nonlinear PV characteristics, changing environmental conditions, and unstable system operating conditions.

3.1. Nonlinearity of PV Characteristics

Nonlinear behavior is a primary PVS characteristic. Power, voltage, and current are three operating source regions that form the current-voltage characteristic. Due to nonlinearity, the voltage-to-current ratio of the PV module changes depending on the voltage or current. The proportional change in voltage with respect to the change in current is called dynamic resistance. Due to the PV module I-V curve linearity in the voltage source region, the dynamic resistance stays constant while being relatively steady in the power region. MPPT is difficult when its function in the current source range is caused by a massive dynamic resistance divergence in the current source region due to significant nonlinearity. The MPP should be operated in the power and voltage regions in order to improve MPPT [116] to better track the maximum power. Based on this phenomenon, the power region should be the region of the MPPT controller adaptation.

3.2. Ambient Condition Variation

The biggest issue with solar systems is that their power output is not continuous and varies depending on the weather [88,117]. One of the biggest issues now is how to adapt MPPT algorithms to rapidly changing environmental conditions. Due to the rapid changes in ambient conditions, numerous MPPT methods are unable to respond to the MPP voltage, which leads to a significant loss. The MPPT must be used to track the voltage at an MPP. The variation in weather conditions has an impact on the PV performance:

- The amount of PV energy depends on the irradiation variation income for horizontal PV arrays.
- The changes in the PV array surface temperature (solar PV cell temperature) affect the amount of energy produced by the PV array.
- Shadowing conditions caused by cloudy weather conditions or a dusty PV array surface can reduce PV power generation [95,96].

According to Figure 1, the higher the temperature of the PV array, the less PV power amount production, where T1 (45 °C) is higher than T2 (25 °C) and T3 (15 °C), so the PV power at T3 and T2 is better than the power at T1. In addition, PV power production is proportional to the solar irradiance values. Indeed, at λ1 (1000 W/m^2), it gives a higher MPP than λ2 (500 W/m^2) and λ3 (100 W/m^2).

3.3. Condition of System Working

The majority of MPPT algorithms use the DC-DC converters as basic and direct resistance transformers with constant efficiency across all levels of voltage. The DC-DC converter, on the other hand, is essentially a non-ideal device that can cause numerous losses. It is important to take this into account. The DC-DC converter efficiency changes according to the duty cycle. The applied converter settling time is a significant determinant of the MPPT effectiveness. MPPT primarily uses current and voltage sampling to determine the power at each step. This power is used to specify the GMPP in advanced methods and to specify the tracking direction in methods such as the P&O method. For the MPPT algorithm, the step size is smaller than the settling time of the boost converter, so the sensed current and voltage values will be incorrect, which will result in wrong PV curve tracking. The controller design needs to be properly considered to prevent instability because V_{mpp} and I_{mpp} must be controlled by the controller duty cycle. Additionally, multiple LMPPs may occur under rapid weather change, as shown in Figure 2 whereas there is only one desired GMPP, with the required MPP indicating the best PV array performance [118].

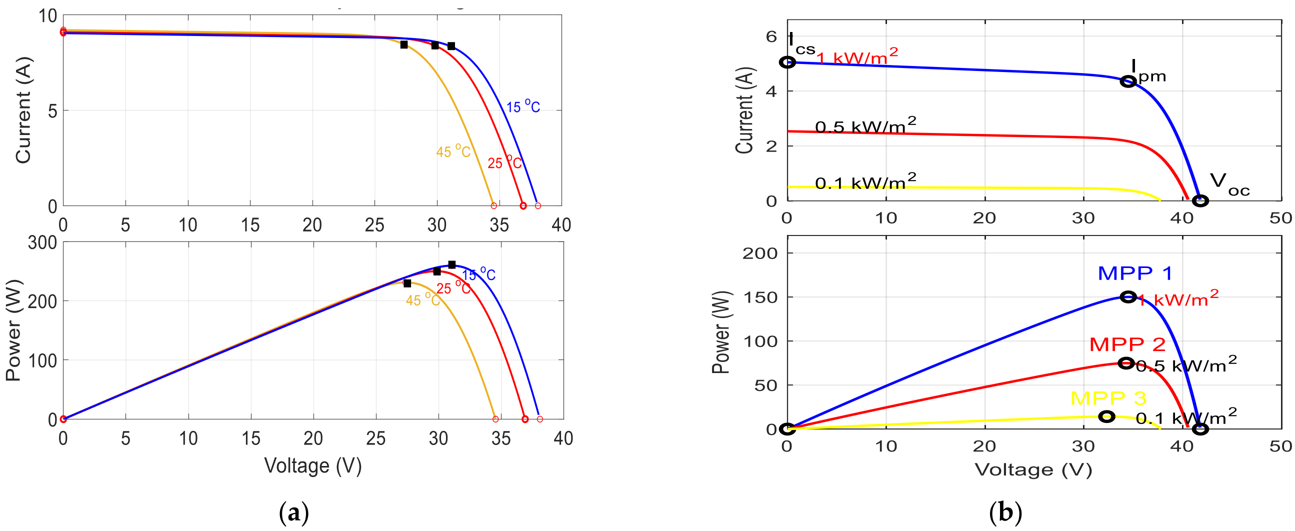

Figure 1. I-V and P-V properties of PV modules at various levels of (**a**) temperature and (**b**) solar irradiation.

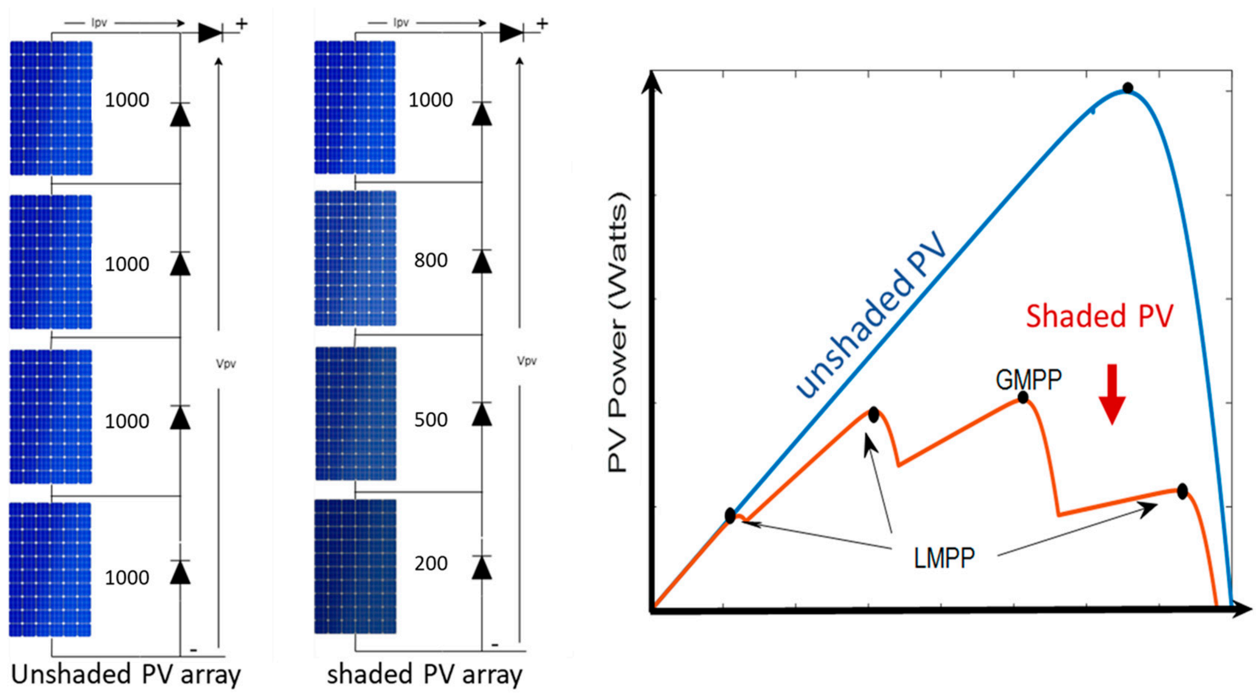

Figure 2. PV panel response under different irradiation conditions.

3.4. Partial Shading Effect on PV Characteristics

When the PV cells do not function under the same irradiation value as under PSCs, causing significant energy losses and having severe effects on PV power generators, and when the electrical characteristics of the PV cells are different, mismatch losses of the PV series connection will be generated.

Under PSCs, in a PV panel, several cells are connected in series to achieve a desired output voltage. If one or more of these cells are shaded, the overall performance of the panel can be significantly reduced. This is because a shaded PV cell produces less current, and since the cells are in series, the current in the circuit is limited by the cell with the lowest current. Thus, even minor shading can have a disproportionate effect on the power output of the panel.

For PSCs, the lowest short-circuit current is observed in PV cells with the lowest irradiance levels. If the shadowed cell current is less than the PV power generator current then the shaded cell starts operating as a load rather than a source, consuming energy instead of producing it. Accordingly, the energy generated by the other cells is lost as heat in that module, resulting in power losses. After that, increasing the cell temperature causes it to suffer irreversible damage. This is the hot spot phenomenon. Next, a bypass diode anti-parallel connected across PV modules is used to overcome this issue. However, these diodes prevent the PV array, under PSCs, from producing the maximum amount of power, and they also make MPPT more complicated by causing multiple local maxima in the P-V characteristic of the PV array. To mitigate the effects of shading, several techniques can be used, such as the use of bypass diodes to avoid shaded cells, or employing optimization techniques for the connection topology of PV cells. More advanced control techniques, such as MPPT algorithms, can also be used to optimize the performance of panels in the presence of shading.

In this study, four PV modules are connected in series and tested under three different irradiation scenarios to evaluate the effect of PSCs on the generation of PV power. The scenarios are as follows:

- Scenario (1): It represents the scenario of uniform irradiation; the four PV modules are exposed to constant irradiation values: 1000 W/m^2. This scenario represents a baseline to evaluate the performance of the proposed method under optimal irradiation conditions.
- Scenario (2): It is a weak shading case; the PV panels are exposed to two irradiance levels: 1000 W/m^2 and 500 W/m^2. This scenario represents a partial shading situation generating two distinct peaks in the power curve: a local peak and a global peak. The main objective of this scenario is to test the MPPT algorithm's ability to avoid becoming stuck on the first local power peak and to correctly track the global power peak (GMPP).
- Scenario (3): It corresponds to severe shading where 1000 W/m^2, 800 W/m^2, 500 W/m^2, and 200 W/m^2 are the four different irradiation levels applied on the four PV modules. The aim of this scenario is to test the MPPT algorithm's ability to correctly identify and track the GMPP among several local peaks.

4. PVS Modeling

The PV array feeds the resistive load using a DC/DC boost converter regulated by MPPT methods. This PVS is depicted in Figure 3. Temperature (T) and irradiance (G) have an effect on the PV array's ability to produce and transfer the most power to the load. This objective is done thanks to MPPT controllers which drive the DC/DC converter by controlling the duty cycle and the pulse generation to fire the DC/DC switch in order to search the MPP.

During simulation, three different irradiation scenarios as inputs to the PV array and three MPPT algorithms are used to control the systems which are P&O, PSO, and CS MPPT controllers. The model used in this work is simulated using Matlab/Simulink.

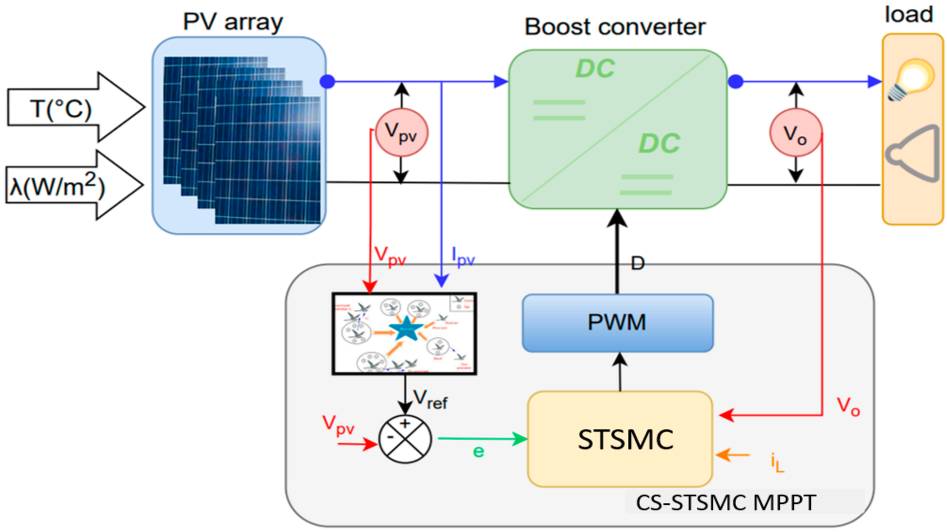

Figure 3. PV system.

4.1. PV Cell Modeling

The basic PVS element is the PV cell, and its equivalent electrical circuit is presented in Figure 4. This model is an electrical PV cell circuit with a single diode. The blue-framed model is viewed as the ideal source of current for producing photocurrent (I_{ph}). It is proportional to the power of incident light. A diffusion current phenomenon (I_d) is produced in parallel by connecting a diode to the current source.

$$I = I_{ph} - I_d, \tag{1}$$

$$I = I_{ph} - I_s\left[\exp\left(\frac{V}{\alpha V_T}\right) - 1\right]. \tag{2}$$

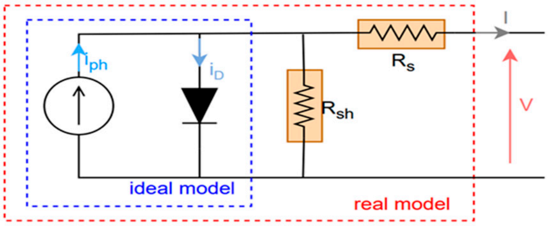

Figure 4. Equivalent electrical PV-cell circuit.

The output current is defined by expression (1), and Equation (2) describes the diode current behavior. However, this expression does not accurately capture how a PV cell behaves. Intrinsic resistance is introduced to properly describe the PV behavior R_{sh}, R_s. A real model is framed in red. The metal contact and the silicon are separated with a contact resistor which is presented by the series resistance R_s. The power loss resulting from manufacturing impacts is presented by a parallel connected resistor called the shunt resistance. Equation (3) presents the PV array model while considering the irradiance and temperature variation to describe the dynamic behavior of the PVS under various weather conditions.

$$I = I_{ph} - I_s\left[\exp\left(\frac{V + I \times R_s}{\alpha V_T}\right) - 1\right] - \left(\frac{V + I \times R_s}{R_{sh}}\right). \tag{3}$$

where I_s is the reverse saturation current of the diode, V_T represents the thermal voltage of the diode, and is described in Equation (4) where the PV cells connected in series are represented as N_s, the Boltzmann constant k is ($1.3806503 \times 10^{-23}$ J/K), T presents the absolute temperature, q is the electron charge (1.60217646 × 10^{-19} C), and α is the diode ideality factor.

$$V_T = \frac{N_s \cdot k \cdot T}{q}. \tag{4}$$

Equation (5) presents the photoelectric current taking into account the variation in atmospheric conditions.

$$I_{ph} = [I_{sc} + K_i(T - T_n)]\frac{G}{G_n}. \tag{5}$$

where I_{sc} is the current of the short circuit at a normal testing condition, the coefficient of the current of the short circuit is presented by Ki (A/K), T (K) defines the actual temperature, and the nominal one is defined by T_n (K). Moreover, the irradiance on the device surface is G (W/m^2), and the nominal irradiance is G_n (W/m^2). The variation in temperature affects the saturation current of the diode, as presented in (6), where E_g is the energy gab, and the nominal saturation current is I_{sn}. The parameters of the PV panel module used in this research work are cited in Table 2.

$$I_s = I_{sn}\left(\frac{T_n}{T}\right)^3 \exp\left[\frac{qE_g}{\alpha K}\right]\left(\frac{1}{T_n} - \frac{1}{T}\right). \tag{6}$$

Table 2. PV module parameters.

Parameters	Values
P_{mp}	150.075 W
V_{mp}	34.5 V
I_{mp}	4.35 A
V_{ov}	41.8 V
I_{sc}	5.05 A

4.2. Boost Converter Sizing and Modeling

The DC/DC boost converter which is the adaptive interface between the PV model and the load is driven by the MPPT controllers. The boost converter is well-known for its improved maximum power transmission with lower energy losses [119]. To increase power transfer, the MPPT algorithm controls the duty cycle of the Pulse Width Modulation (PWM) signals. Accordingly, a DC-DC boost converter is used in this study for better conversion efficiency. To lower the power losses at a higher frequency, the MOSFET, which is categorized as a switching device, is controlled by the PWM.

Equations (7) and (8) describe the relations between the converter input and output voltage and the converter input and output current, respectively.

$$V_o = V_{pv}\frac{1}{1 - d}, \tag{7}$$

$$I_o = I_{pv}\frac{1}{1 - d}. \tag{8}$$

4.2.1. Capacitor C_{in} Design

Typically, the aim of capacitors is to satisfy the energy needs during transient periods such as sudden load or irradiation changes. Equation (9) is used to create the DC-link capacitor that is connected in parallel to the PV array.

$$C_{in} = \frac{1}{2}C_{in}\left[V_{PV}^2 - V_{min}^2\right] = P_{PV} \times \Delta t. \tag{9}$$

where, the minimally allowable voltage of the PV is V_{min}, the transient time is presented by Δt, and V_{PV} is the PVS voltage. The system switching frequency (f_s) is 50 kHz. The parameter C_{in} is equal to about 80 µF when V_{PV} is set to the framework voltage of a PV array at an MPP of (138 V), V_{min} is set to half of that voltage (69 V), and Δt is set to three times the switching period.

4.2.2. Output Filter Capacitor Design C_{out}

The DC/DC boost converter output voltage V_{out} is controlled at a particular value. This value is taken to be double the framework voltage for a PV array at an MPP for design procedures. When there is a decrease in irradiance or there is significant partial shading, the output filter capacitor supplies the load energy. Therefore, Δt is assumed to have a time of 1 ms. With V_{min} at 69 V and P_{PV} at 600 W, the same general equation from Equation (9) yields a value for C_{out} of at least 20 µF [87].

4.2.3. Inductance Design of Boost Converter

Equation (10) defines the maximum duty cycle value and Equation (11) presents its minimum value. These values have to be calculated to design the inductance of the boost converter.

$$D_{max} = \frac{V_o - V_{PV,max}}{V_o}, \quad (10)$$

$$D_{min} = \frac{V_o - V_{PV,min}}{V_o}. \quad (11)$$

$V_{PV,min}$ and the minimum duty cycle are used to ensure the current of the PV array in a continuous mode of conduction [31]. The inductance value is therefore given in (12).

$$L = \frac{P_{PV} \times D_{min}}{\Delta I_{PV} \times f_s}. \quad (12)$$

4.2.4. Equivalent Design of Load Resistance

By neglecting the losses of the boost converter and the PV module, the output and input power capacity (600 W) are equal, resulting in an equivalent load resistance according to (13).

$$R_L = \frac{V_o^2}{P_{PV}}. \quad (13)$$

The dynamic state of the boost converter in terms of the duty cycle "D" can be depicted using the averaging method [120]. The DC/DC boost converter parameters are summarized in Table 3.

$$\begin{cases} \dfrac{dV_{pv}}{dt} = \dfrac{i_{pv} - i_L}{C_{in}} \\ \dfrac{di_L}{dt} = \dfrac{V_{pv} - V_o + D \cdot V_o}{L} \end{cases}. \quad (14)$$

Table 3. Boost converter parameters.

Parameters	Values
Inductance L	1.38 mH
Capacitor C_{in}	80 µF
Capacitor C_{out}	20 µF
Load resistance R_{load}	119 Ω

5. MPPT Algorithms

The incident energy consumed by the PV panel is between 35% and 45%, and it is then transformed into electrical energy, according to various literature studies. The maximum PV power is extracted using MPPT controllers by determining I_{mpp} and V_{mpp} at various climatic conditions in order to improve the PVS power generation efficiency [121]. In this work, in order to track the MPP, the P&O, PSO and CS, CS-PID, and CS-STSMC-based MPPT algorithms are employed.

5.1. P&O Algorithm

P&O is the most popular MPPT technique. The PV current and voltage are measured periodically to calculate the PV power. By changing the duty cycle of the DC-DC converter, it then offers the operating voltage perturbation steps based on the power change. To evaluate the power change ΔP, the PV output power for each iteration is compared with that of the step before. Depending on the sign of (ΔP/ΔV), the voltage perturbation sign is defined and the duty cycle will either increase or decrease [122,123].

The perturbation step size selection is the key component of this algorithm. If it is large, convergence occurs quickly, but it results in significant oscillations in the power of the steady state. Inversely, it will result in unwanted losses of PV power. This technique has undergone numerous modifications to speed up convergence and minimize oscillations regarding the MPP. Using a variable step size is one of these modifications [124]. In uniformly distributed irradiance, this technique performs well, but in PSCs, it may become stuck at one of the LMPPs. Because of this, numerous initiatives to enhance the P&O controller in the case of PSCs have been published in the literature [125]. One of these methods involved forcing standard P&O to operate around the operating voltage value with the highest power by scanning values. This method successfully captures the GMPP location in PSCs within a reasonable limit, but it lengthens the convergence time.

5.2. PSO-MPPT Algorithm

Eberhard and Kennedy were the two researchers who created the intelligence optimization theory known as PSO. They used this phenomenon to solve the issues with search and optimization. The feeding habits of birds and schooling fish served as the inspiration for this algorithm's basic idea [126]. In fact, this method employs a number of cooperating birds, also known as particles. Each particle has a unique fitness value that is defined by an objective function, where velocity is utilized to establish the movement direction and range. Each particle offers the knowledge it has learned via its own particular search process. Figure 5 illustrates the particles movement.

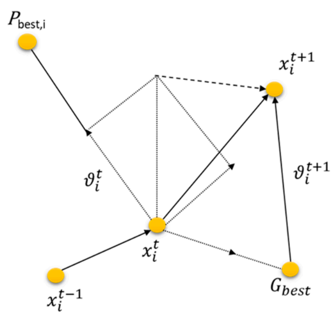

Figure 5. Particle movement in PSO-MPPT algorithm.

Each particle's best location is saved by P_{best} as the greatest individual position. By comparing the particle swarm's individual positions, G_{best}, is found and saved as the swarm's best position, which has an impact on the movement of particles. This process is used by the particle swarm to constantly adjust its direction and speed as it moves in the direction of the ideal location. Each particle converges with high speed to a closely optimal position in this way. The standard PSO method is defined by Equations (14) and (15).

$$V_i(k+1) = \omega\ V(k) + c_1\ r_1(P_{ibest}(k) - P_i(k)) + c_2\ r_2(G_{best}(k) - P(k)), \quad (15)$$

$$P_i(k+1) = P_i(k) + V_i(k+1). \quad (16)$$

where V_i defines the velocity of particle i, P_i presents the position of particle i, k is the number of iterations; ω the inertia weight; r_1 and r_2 are random variables and their values are between [0, 1], c_1 is the cognitive coefficient, c_2 defines the social coefficient, P_{ibest}

presents the individual particle is the best position, and G_{best} defines the particle swarm's best position.

What follows is an explanation of this method's fundamental operating concept as depicted in Figure 6:

- Step 1: Initialization of PSO parameters: Each particle velocity and position are initialized randomly in a uniform distribution over the search space for this MPPT algorithm, where the fitness value evaluation function is the generated output power and the particle position is the converter duty cycle;
- Step2: Fitness evaluation: Following the controller transmission of the command of the duty cycle instruction, which denotes particle i, the fitness value is determined;
- Step3: Global and individual best data update: Using a comparison between the recently computed fitness values with the previous ones, individual and global best fitness values (P_{ibest} and G_{best}) and positions are updated. Moreover, G_{best} and P_{ibest} as well as their appropriate positions are replaced as needed.
- Step4: Updating each particle's velocity and position: The position and velocity of each particle swarm are updated using Equations (15) and (16).
- Step5: Convergence evaluation: The convergence criteria are examined. If the latter is satisfied, then the process can be finished; else, the number of iterations will go up by 1 and the next step will be taken;
- Step6: Re-Initialization: In the conventional PSO method, the convergent criteria are either to find the best solution or to complete the iterations. The fitness value, however, varies with the load and weather in PV systems, so it is not constant. As a result, whenever the PV module output changes, PSO needs to be re-initialized and to search for a new MPP.

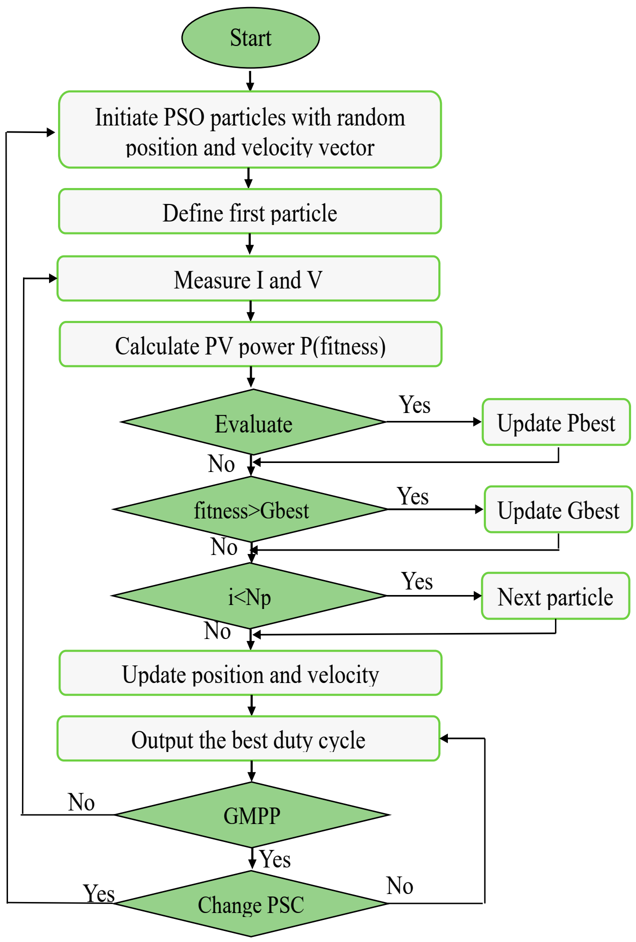

Figure 6. PSO-MPPT algorithm.

This method is an efficient method in tracking the MPP even under PSC, but it takes a long time to track the GMPP. Besides, this method uses three tuning parameters that make it more complex.

5.3. CS-MPPT Algorithm

Due to the captivating sounds and aggressive reproduction methods of cuckoo birds, some varieties of them include the ani and the guira. The eggs of these species are laid in collective nests and may take eggs from other nests to improve the chances that their eggs will grow. Some cuckoo birds engage in brood parasitism. These intelligent birds, known as Tapera, imitate their host shapes and colors, which may increase the likelihood of successful reproduction. Observing the rhythm of Tapera's egg-laying is awe-inspiring and gorgeous.

In order to select the best nest, a host species group with similar nesting places and egg traits is the primary choice of cuckoo females. Foreign eggs can be deceived into being taken by host birds. However, if any are found, they are either thrown outside the nest or the entire nest is destroyed. Then, the host bird moves on to build a new nest somewhere else. There exist three main brood parasitism types: intraspecific, cooperative, and nest takeover.

5.3.1. Lévy Flight

Finding the best nest is where cuckoo birds begin, but this process is crucial to the reproduction of cuckoo birds. The method of looking for food and looking for a nest is the same. Lévy flight is a well-liked model, and it serves as the basis for the selection and modeling of walks and routes. Fruit flies, or Drosophila melanogaster, employ a succession of straight flight routes interspersed with sudden 900-degree twists to investigate their environment, according to new research by Reynolds and Frey. This behavior is applied when creating optimizations for various issues [127]. Levy flight defines a type of random walk where the step lengths have a probability distribution Pa. For CS, in Equation (17), the step length is calculated based on the power law of the Levy distribution [44].

$$\text{Levy} \sim u = t - \lambda \text{ where } (1 < \lambda \leq 3). \tag{17}$$

Here, a random walk process with a heavy-tailed power-law step-length distribution is based on these steps.

5.3.2. CS-MPPT Algorithm

The CS algorithm adheres to three key rules:

- Each cuckoo will only lay one egg during a single iteration, and it will be laid in a randomly chosen nest.
- Only the next generation may make use of the surrogate bird nests that produce the highest-quality eggs.
- The total surrogate nests' cumulative values are preset, and only a cuckoo may lay the considered egg and a specific probability will be assigned if the surrogate bird is found.

It is possible for the host bird to eat the cuckoo eggs or to destroy its nests if it knows that the cuckoos' eggs are there. There is also a likelihood of Pa that a new nest will be created. The final supposition may be approximated in its simplest form by the Pa fraction. After that, the new nests replace the n nests with new random solutions. Each egg is a potential approach, and a cuckoo egg is used to depict a novel solution, as explained in the following representation. Foreign egg discovery will be to select a few bad nests that contain unbeatable results. Consequently, the solutions which are discovered will be taken into account for future results and calculations.

Levy flight is carried out while creating a new solution $X\ (t+1)$ for cuckoo i.

$$Xi(t+1) = Xi(t) + \alpha \oplus \text{levy flight}\ (\lambda). \tag{18}$$

where $\alpha > 0$ is the step size linked to the optimization problem scales. It is usually, considered that $\alpha = 1$. In Equation (18), the current position is presented by the first term and the transition probability is presented by the second component. Multiplication in the entry order is indicated by product $\oplus$.

The search mechanism flowchart of the CS controller is illustrated in Figure 7. First, the initial duty cycle number is chosen randomly, and then it is used on PV panels. Second, to estimate PV power, the system voltage and current are determined. Such a strength exemplifies the fitness value. After that, the current best nest is determined to be the duty cycle for the optimal fitness function (d_{best}). Next, new nests are created using Levy flight, based on Equation (17). Fourth, the PVS is used to evaluate the values of new finesses. Then, with a chance of Pa, the worst nest is randomly demolished, simulating the host bird's behavior of finding and destroying the egg of the cuckoo. Afterward, the destroyed nest is changed with the new one using a levy flight, followed by measurements of the PV power and the selection of the best nest at the time. Finally, the CS controller stops once the stopping criteria are satisfied and the CS algorithm succeeds in tracking the global point by providing the best duty cycle.

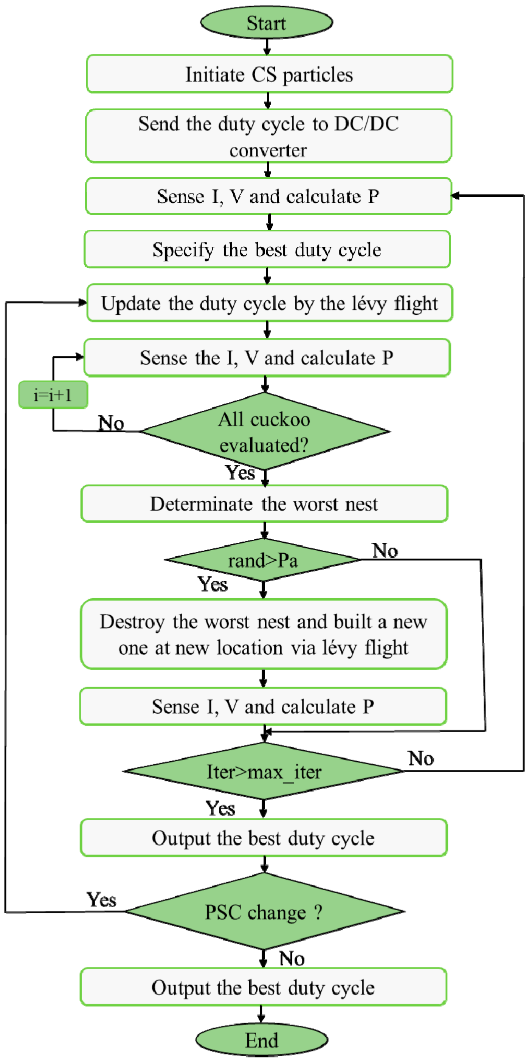

Figure 7. CS-MPPT algorithm.

5.4. Hybrid CS-MPPT Algorithm

Referring to the literature review, the hybrid CS-MPPT method is based on the combination between the CS algorithm and a PID controller [42]. The aim of this combination is to exploit the strengths of both techniques while avoiding their respective drawbacks. Thus, CS is renowned for its efficiency and rapid convergence in extracting the GMPP. The inputs of the CS algorithm are the voltage and current of the PVS, and its output is the reference voltage 'V_{ref}' which allows the panel to operate at its MPP. Then, the generated 'V_{ref}' is subtracted from the PV voltage, and the difference is routed to the PID controller. This technique reduces the percentage of error (e) generated by the conventional CS-MPPT algorithm, and it increases the PV system efficiency by providing an accurate value of the converter duty cycle. Next, a regulator output determines the amount of the duty cycle to apply to the PWM to regulate the input voltage. The PID controller is advantageous for its ability to minimize overshooting during transitions and to increase stability during continuous operations. However, introducing the derivative term into the controller can result in unwanted input noise, which can potentially disturb the output voltage. In this work, the parameters of the PID controller are fine-tuned using a trial-and-error approach, which is not a successful approach. The PID controller is an effective solution for improving the performance of the CS-MPPT algorithm, provided that the coefficients are correctly adjusted.

This problem is solved with the employment of SMC in combination with the CS-MPPT algorithm. In this context, and in order to overcome this problem, the PID controller is replaced by STSMC, which will be synthesized in the following subsection.

5.5. Proposed CS-STSMC-MPPT Algorithm

The SMC control technique is considered a variable-structure technique and is widely used in various applications. It is recognized by its robustness in the face of uncertainties and external disturbances, as well as for its ease of design and implementation [128]. The SMC strategy consists of making the system trajectory move along a predefined switching surface under the effect of a specific control law. The SMC principle forces the system trajectory to slide along a switching surface under a determined control law. It is basically composed of two phases: a reaching phase where the state trajectory is driven to the surface S = 0 and reaches it in a finite time, followed by a sliding phase where it slides on the switching surface to an equilibrium point.

The operating principle of SMC can be enveloped in the following tasks:

- Selection and design of a sliding surface,
- Formulation of a control law that compels the system state trajectory to converge to a pre-specified surface within a finite timeframe,
- Sustainment in the vicinity of this surface by employing a suitable switching logic.

To achieve high-performance controlan requires accurate and high-speed tracking, an integral and derivative sliding surface "*s*" can be chosen, where the derivative and the integral terms were used to eliminate the overshoot and minimize the error in steady-state conditions. The sliding surface "*s*" is expressed as follows:

$$s(t) = a\dot{e}(t) + e(t) + b\int e(t)\mathrm{dt} \tag{19}$$

where "$e(t)$" represents the voltage error calculated by subtracting V_{pv} from V_{ref}, while "$\int e$" is the integral term and $\dot{e}(t)$ is the derivative term of the error. The parameter "a" and "b" denote the sliding surface coefficient.

Usually, the SMC is composed of two components, the equivalent control law and the discontinuous control action, as written in Equation (19):

$$u = u_{eq} + u_{dis} \tag{20}$$

The sliding surface derivative is "$\dot{s}$", to obtain u_{eq}, the time derivative of Equation (15), and set it to zero as follows:

$$\begin{aligned} \dot{s} &= a\ddot{e}(t) + \dot{e}(t) + be(t) = 0 \\ &= a\ddot{v}_{pv} + \dot{v}_{pv} + be(t) = 0 \end{aligned} \tag{21}$$

By substituting (14) in Equation (20), it is possible to yield Equation (21):

$$-\frac{a}{C_{in}}\left(\dot{i}_{pv} - \dot{i}_L\right) - \frac{1}{C_{in}} i_{C_{in}} + be(t) = 0 \tag{22}$$

where $i_{C_1} = \dot{i}_{pv} - \dot{i}_L$, by using Equation (14), Equation (21) can be rewritten as:

$$-\frac{a}{C_{in}}\left(\dot{i}_{pv} - \frac{1}{L}(v_{pv} - v_o + v_o D)\right) - \frac{1}{C_{in}} i_{C_{in}} + be(t) = 0 \tag{23}$$

Consequently, the formulation of the equivalent control law u_{eq} can be expressed as follows:

$$u_{eq} = D_{eq} = \frac{1}{v_o}\left(v_o - v_{pv} + \frac{L}{a} i_{c_{in}} + L\dot{i}_{pv} - \frac{bC_{in}}{a} Le(t)\right) \tag{24}$$

The discontinuous component, denoted as u_{dis} is employed to compel the sliding mode to adhere to the sliding surface, which is traditionally expressed in the following manner:

$$u_{dis} = -K_1 \cdot \mathrm{sign(s)} \tag{25}$$

where, K_1 represents the proportional gain associated with the discontinuous control, and sign(s) denotes the sign function. The discontinuous switching control, u_{dis}, is crucial for accommodating external disruptions.

The HOSMC strategy maintains the efficacy of the FOSMC approach while eliminating the chattering phenomenon [57]. However, it is based on higher-order derivatives of the sliding surface. The STSMC belongs to the SOSMC category and operates only based on the sliding surface "s", without requiring the derivative of "s". The discontinuous term of the proposed super-twisting controller can be defined by the function U_{ST}, which is constituted by two components as shown in Equation (26) [56,129]:

$$u = u_{ed} + u_{ST} \tag{26}$$

where u_{ST} is defined with Equation (27):

$$\begin{cases} \dot{u}_1 = -K_1 sign(s) \\ u_{ST} = -K_2 |S|^{\alpha} \cdot sign(s) + u_1 \end{cases} \tag{27}$$

The positive constants K_1 and K_2 are employed to formulate robust STSMC. Meanwhile, parameter α denotes the level of non-linearity, typically restricted within the range "$0 \leq \alpha \leq 0.5$." In most scenarios, this parameter is set equal to 0.5 [130]. The necessary conditions to ensure finite time convergence are as follows [57]:

$$\begin{cases} K_1 > \dfrac{\phi}{\Gamma_m} \\ K_2 \geq \dfrac{4\phi}{\Gamma_m^2} \dfrac{\Gamma_M \cdot (K_1 + \phi)}{\Gamma_m (K_1 - \phi)} \end{cases} \tag{28}$$

where K_1, K_2, ϕ, and Γ_m are chosen as positive constants [57]. Finally, the Duty cycle "D" generated by the proposed STSMC is given by Equation (29):

$$D = D_{eq} + U_{ST} \tag{29}$$

6. Simulation Results and Discussion

In this work, a comparison between three MPPT controllers is done. The proposed CS-STSMC-MPPT algorithm is compared to CS-PID, CS, PSO, and P&O MPPT methods under three different partial shading cases which are simulated using the MATLAB environment, in order to test the efficiency of the proposed CS-STSMC-MPPT algorithm in reducing the negative impact of PSCs on the maximum power production in standalone PVSs, as shown Figure 8.

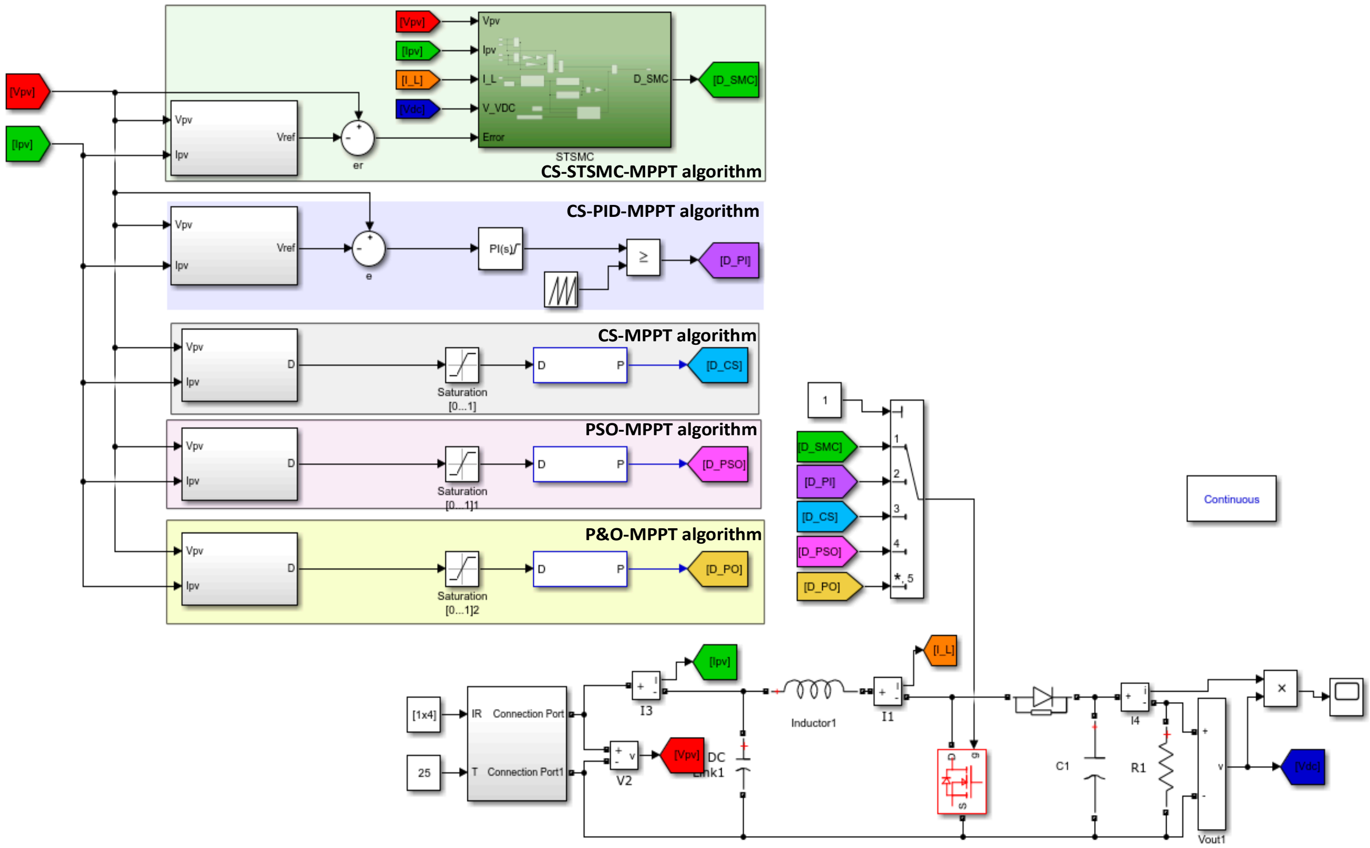

Figure 8. System overview.

This system is composed of four PV modules connected in series and a boost converter driven by MPPT controllers to supply a resistive load. The parameters of the simulated system are illustrated in Tables 2 and 3.

In this work, the used MPPT algorithms are CS-STSMC, CS-PID, PSO, CS, and P&O MPPT algorithms. Parameters of PSO, P&O, and CS algorithms are summarized in Table 4. Their performance is tested, under different weather conditions. The first scenario presents uniform irradiance, and the second and third ones present partial shading, as provided in Table 5. Figure 9 presents the response of the PV panel under PSCs. The first curve describes the first case of irradiation conditions, and the second and third curves show the second and third irradiation scenarios, respectively.

Table 4. MPPT controller's parameters.

P&O Parameters	PSO Parameters	CS Parameters
$D_{init} = 0.7$	$\Omega = 0.2$	$\lambda = 1.5$
$\Delta D = 0.0001$	$c1 = 0.8$	$\alpha = 0.75$
	$c2 = 1$	

Table 5. Studied cases.

Case Study	Irradiance of Each Module				GMPP
	PV1	PV2	PV3	PV4	
Case 1	1000	1000	1000	1000	600.3
Case 2	1000	1000	500	500	326.1
Case 3	1000	600	500	300	244.83

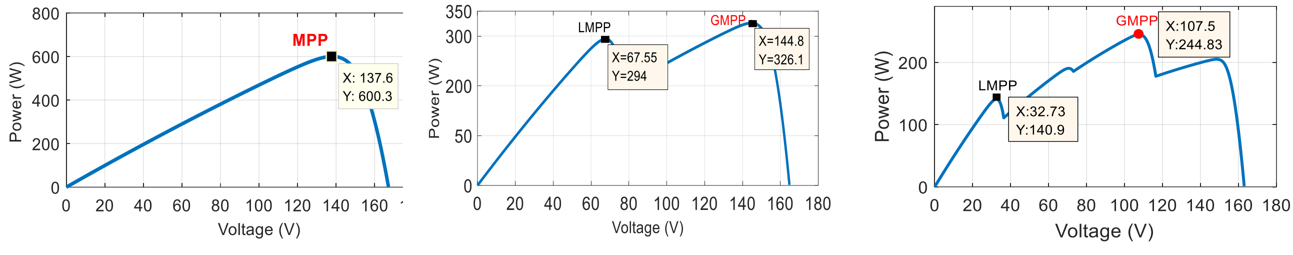

(**a**) (**b**) (**c**)

Figure 9. P-V characteristic under (**a**) case 1, (**b**) case 2, and (**c**) case 3.

6.1. First Case (Case 1)

The four PV modules are subjected to uniform irradiation of 1000 W/m^2. This means that each module receives the same level of irradiation. There exists only one peak at 600.3 W on the P-V characteristic. The simulation results of P&O, PSO, CS, CS-PID and the proposed CS-STSMC MPPT techniques are depicted in Figure 10a,b,c,d,e respectively.

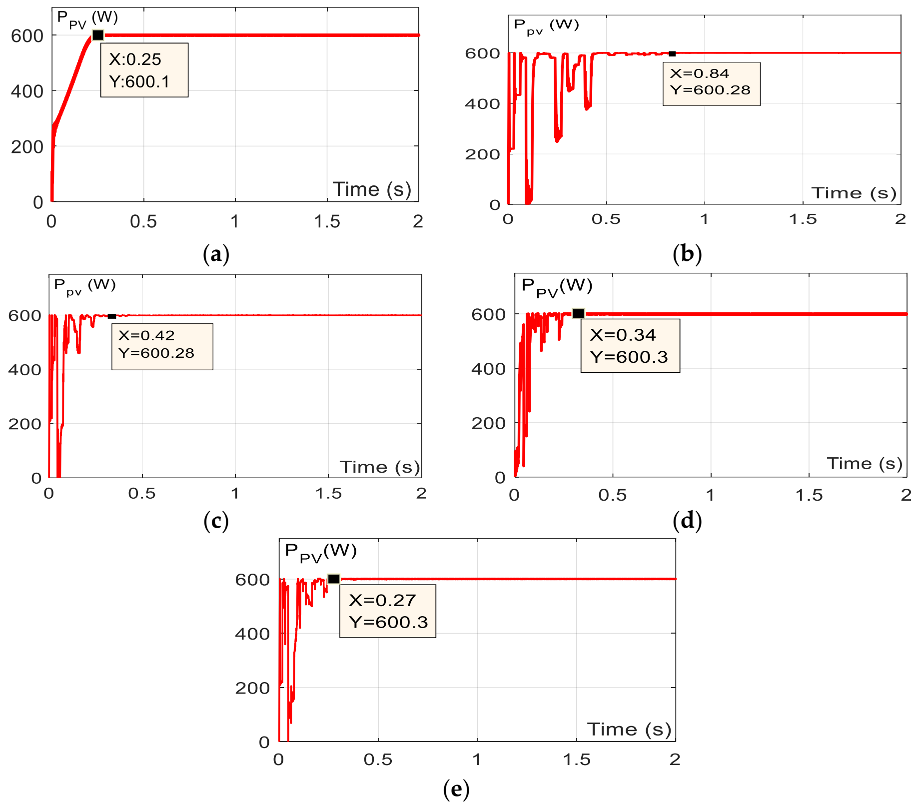

Figure 10. PV power system responses using (**a**) P&O (**b**) PSO (**c**) CS (**d**) hybrid CS-PI, and (**e**) CS-STSMC MPPT controllers under Case 1.

Figure 10a shows the time response of the power delivered by the PVS when P&O is applied. This curve shows a rapid increase in power as the system approaches the MPP, reaching 600.1 W in 0.25 s. It is worth noting that the response has high fluctuations which are between 600.1 W and 599.3 W, which indicates that this method is not perfectly stable when operating near MPP when the steady state accuracy of the PVS is about 0.12%, which is high. In fact, these oscillations are the characteristics of the P&O-MPPT method as it continuously perturbs the system to maintain the MPP. Nevertheless, they can cause power losses that can affect the efficiency of this method. The accuracy of the PSO, CS, CS-PID, and proposed MPPT algorithms is high and the fluctuation is negligible, compared to P&O as shown in Figure 10b,c, respectively. It can also be noticed that the CS and PSO MPPT algorithms achieve the same value of the MPP which is 600.28 W. Figure 10d,e shows that CS-PID and CS-STSMC-MPPT algorithms achieve 600.3 W, which is the GMPP with 100% efficiency. In this context, the traditional P&O technique excels in quickly extracting the GMPP. The hybrid CS-PID and CS-STSMC approaches, demonstrate improved speed when compared to conventional CS and PSO-MPPT. Notably, the proposed CS-STSMC-MPPT algorithm achieves the global maximum in 0.27 s, marking a significant improvement over other methods.

Figure 11a shows the PV voltage response with the P&O-MPPT algorithm. The steady-state voltage value is equal to 138 V with noticeable oscillations around this value that varies between 139 V and 137 V. Figure 11d,e show that the PV voltage of the CS-PID and the proposed CS-STSMC-MPPT algorithms accurately and rapidly pursue Vref. Through Figure 11d, we remark voltage ripples that present the disturbance caused by the unwanted input noise caused by the derivative term of the PID controller. The proposed algorithm reduces the voltage ripples compared to the CS-PID MPPT algorithm. Additionally, according to Figure 12a, the PV current of the P&O-MPPT algorithm is equal to 4.35 A after 0.25 s with many oscillations around this value. Figure 11b,c show the time evolution of the PVS voltage when the PSO and CS MPPT algorithms are applied. For the PSO-MPPT algorithm, the voltage value corresponding to the MPP is 137.98 V and the CS-MPPT algorithm reaches 136.37 V with a slight fluctuation afterward. Figure 12b shows the PV current response which stabilizes at 4.3505 A for the PSO-MPPT algorithm. For the CS-MPPT algorithm, Figure 12c shows that the curve stabilizes at the value of 4.4018 A. Figure 12d,e presents the PV current responses for the CS-PID and CS-STSMC MPPT algorithms.

6.2. Second Case (Case 2)

Case 2 is the scenario of weak shading. Each two PV panels are exposed to an irradiation value. The first two panels are exposed to 1000 W/m^2, and the other two panels are exposed to 500 W/m^2. As a result, two peaks are shown in the P-V curve, as depicted in Figure 9b. The first peak is an LMPP equal to 294 W, and a GMPP at 326.1 W is the second peak.

Figure 13e shows the simulation of the proposed CS-STSMC-MPPT algorithm. This algorithm reaches the GMPP after 0.43 s with high efficiency. The proposed algorithm is faster than the CS-PID algorithm, which converges to a global point after a time of 0.56 s with an oscillation around the GMPP, as shown in Figure 13d. Figure 13c displays the simulation of the CS-MPPT algorithm. It is observed that after a convergence time of 0.59 s, the MPP is reached, with negligible oscillations around it. On the other hand, the PSO-MPPT algorithm reaches 326 W after 1.15 s, as depicted in Figure 13b. The steady-state precision of the PSO-MPPT algorithm is too low. The CS-MPPT algorithm performs better than the PSO-MPPT algorithm in terms of convergence speed and accuracy. Moreover, the hybrid CS-PID algorithm and the proposed CS-STSMC-MPPT algorithm present superior performance in terms of efficiency and rapidity compared to CS and PSO. We can notice that the proposed CS-STSMC-MPPT algorithm improves the convergence time by 23.2%, 27.12%, and 62.6% compared to CS-PID, CS, and PSO.

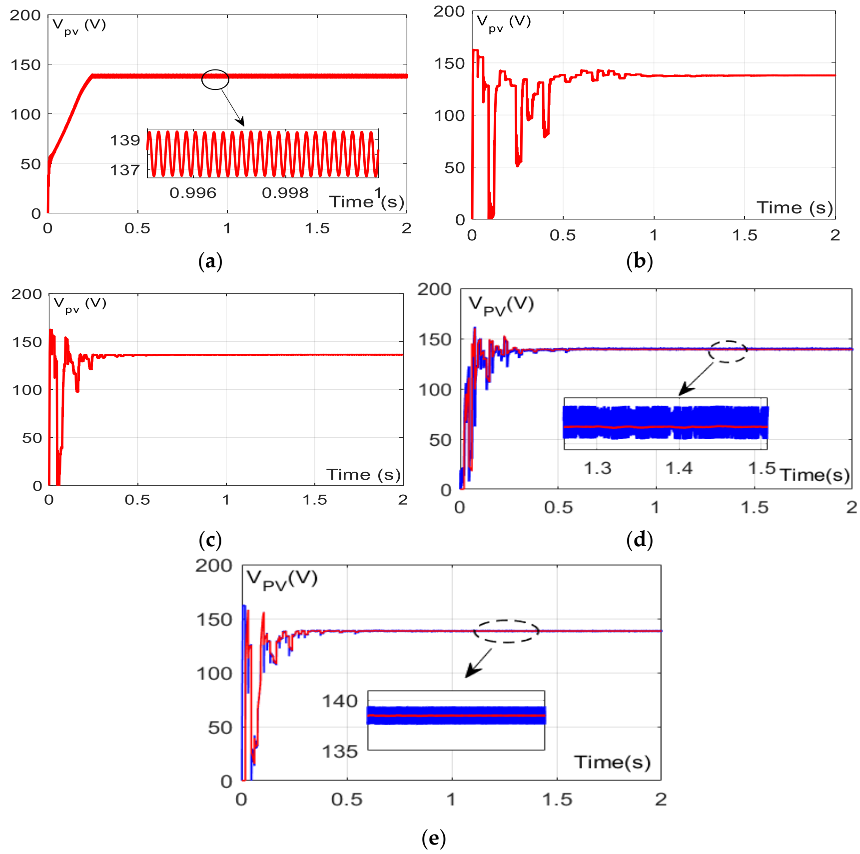

Figure 11. PV voltage using (**a**) P&O, (**b**) PSO and (**c**) CS (**d**) CS-PID, and (**e**) CS-STSMC MPPT methods.

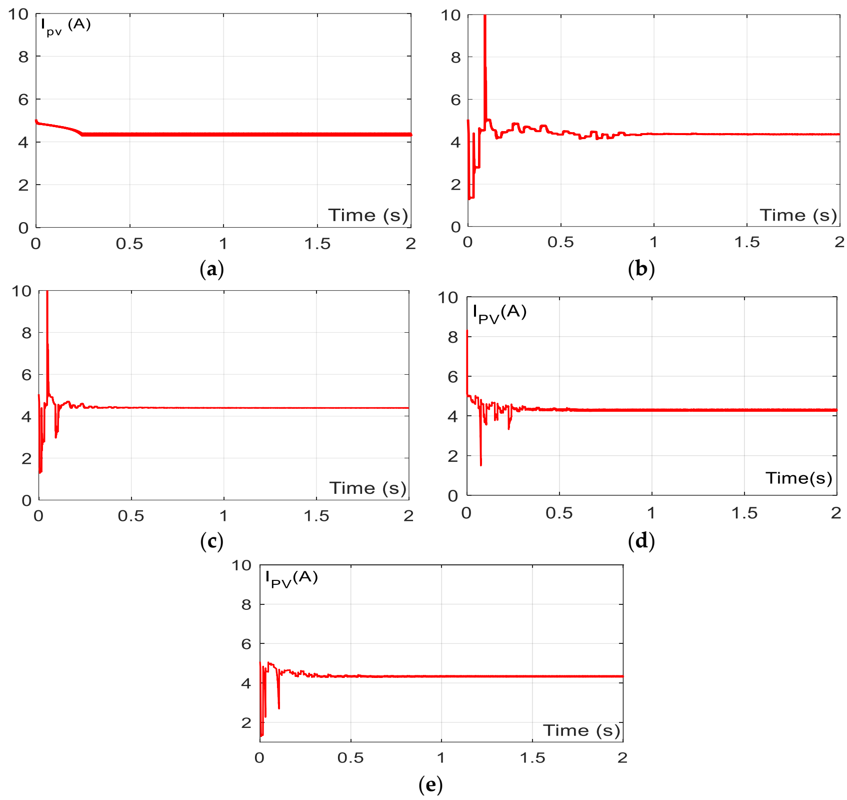

Figure 12. PV current using (**a**) P&O, (**b**) PSO and (**c**) CS (**d**) CS-PID, and (**e**) CS-STSMC MPPT controllers.

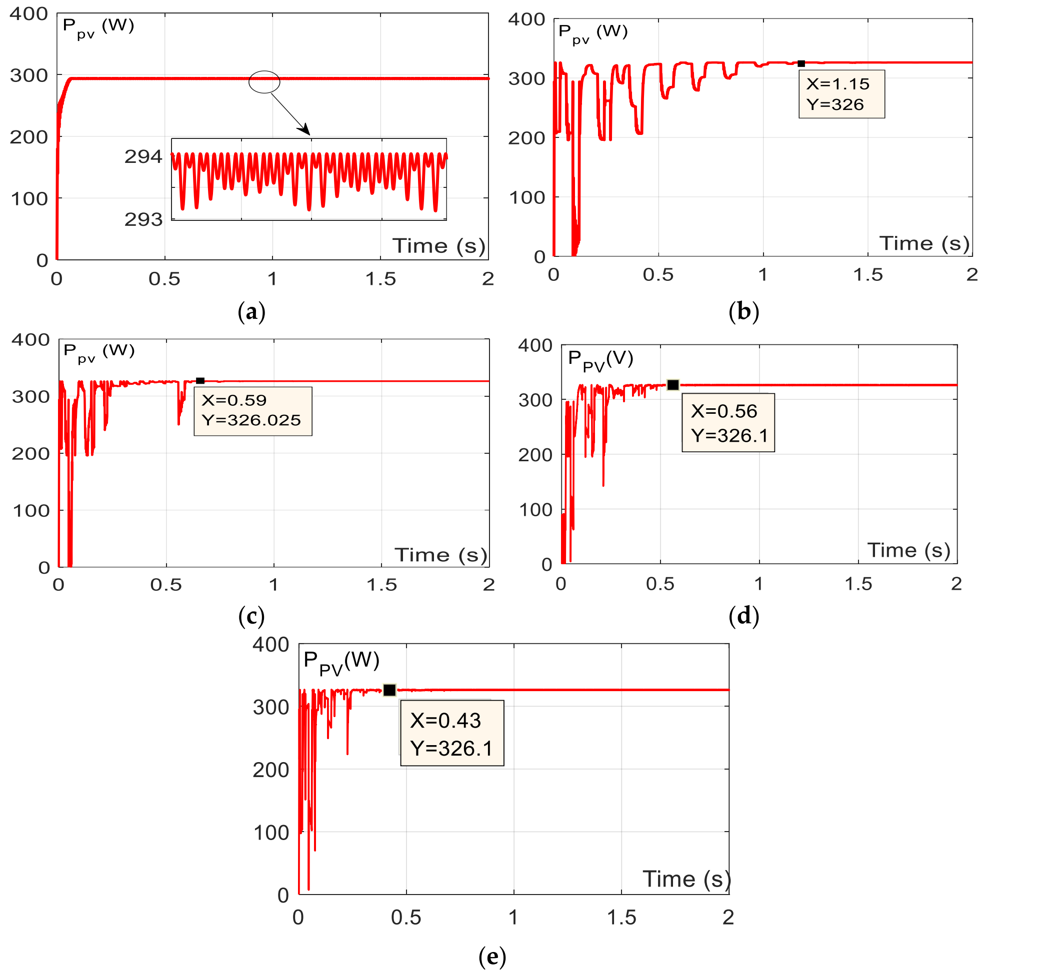

Figure 13. Simulation results of PV power using (**a**) P&O, (**b**) PSO and (**c**) CS (**d**) CS-PID (**e**) CS-STSMC MPPT algorithms under Case 2.

However, the P&O-MPPT method is unable to track the GMPP and becomes stuck at the LMPP, exhibiting large oscillations around this value with 0.25% precision. This precision is considered high compared to the PSO and CS MPPT algorithms.

Figure 14 shows the response of the PV voltage for the P&O-MPPT algorithm, which stabilizes at a value of 67.59 V with significant oscillations. Figure 14b,c displays the PV voltage responses when applying the CS and PSO MPPT algorithms, respectively, which stabilize at values of 144.73 V and 144.7 V. In Figure 14d,e, the curve in blue presents the PV voltage, which follows rapidly and accurately the curve in red which is the V_{ref} curve. Figure 14d,e show that the PV voltage of CS-PID and CS-STSMC-MPPT algorithms purse accurately and rapidly the V_{ref}. Through Figure 14d, we remark voltage ripples which present the disturbance caused by the unwanted input noise caused by the derivative term of the PID controller. The proposed algorithm reduces the voltage ripples compared to the CS-PID MPPT algorithm. The evolution of the current is presented in Figure 15.

6.3. Third Case (Case 3)

Case 3 is weak shadowing, where the four PV modules are exposed to four different irradiation values: 1000 W/m^2, 600 W/m^2, 500 W/m^2, and 300 W/m^2. Figure 9c demonstrates that this case gives four peaks on the P-V curve: The third peak presents the GMPP at 244.83 W. Figure 16 provides the simulation responses of each algorithm. The CS-MPPT algorithm reaches 244.8 W after 0.65 s as illustrated in Figure 16b,c shows that the PSO-MPPT algorithm takes a longer time to attain the GMPP. The proposed CS-STSMC-MPPT algorithm is the fastest algorithm in tracking the GMPP, and it reaches 244.83 W in

0.58 s with low oscillations around GMPP as illustrated in Figure 16e. Figure 16 presents the efficiency of the CS-PID-MPPT algorithm in tracking the GMPP with a convergence time of 0.62 s. However, P&O is fooled by the local maximum and displays significant fluctuations close to it with 1.32% of accuracy which is considerable compared to the PSO and CS-MPPT algorithms. We can interpret that the CS-STSMC-MPPT algorithm is faster and more precise than the other algorithms for this case.

Figure 17a shows the response of the PV voltage for the P&O-MPPT algorithm, which stabilizes at a value of 32.5 V with significant oscillations, and Figure 18a is the curve of current response that stabilizes at 4.43 A. Furthermore, the PVS stabilizes at a voltage of 109.38 V and a current of 2.24 A when the CS-MPPT algorithm is applied, as it is depicted in Figures 17c and 18c. Figure 17d,e shows the PV voltage for the CS-PID and the proposed CS-STSMC-MPPT controllers. We remark that the CS-STSMC-MPPT algorithm reduces the ripples in the PV voltage curve for the CS-PID MPPT algorithm. Therefore, the proposed CS-STSMC-MPPT algorithm can reduce the problem caused by CS-PID. The PV current responses for the proposed CS-STSMC-MPPT algorithm and CS-PID-MPPT algorithm as shown in Figure 18d,e, respectively.

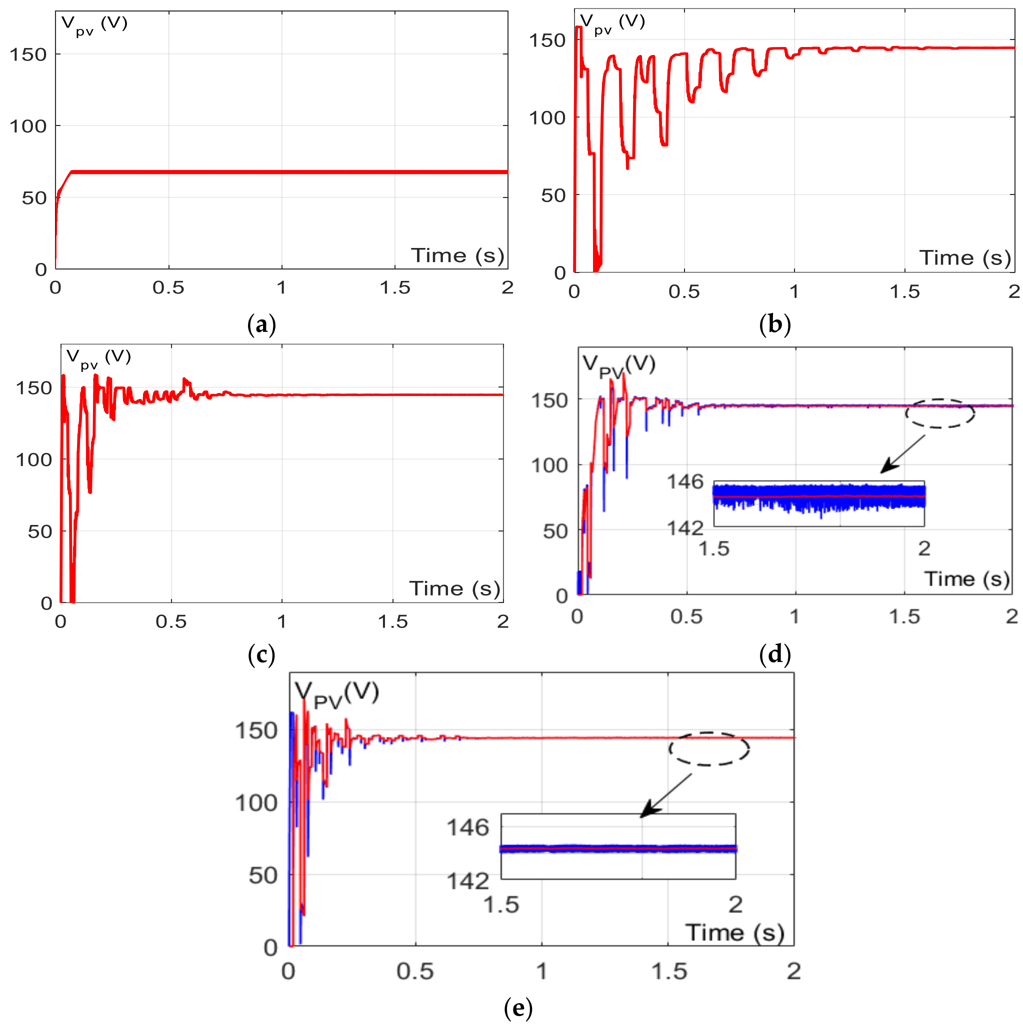

Figure 14. PV voltage using (**a**) P&O, (**b**) PSO, (**c**) CS (**d**) CS-PID, and (**e**) CS-STSMC MPPT algorithms under Case 2.

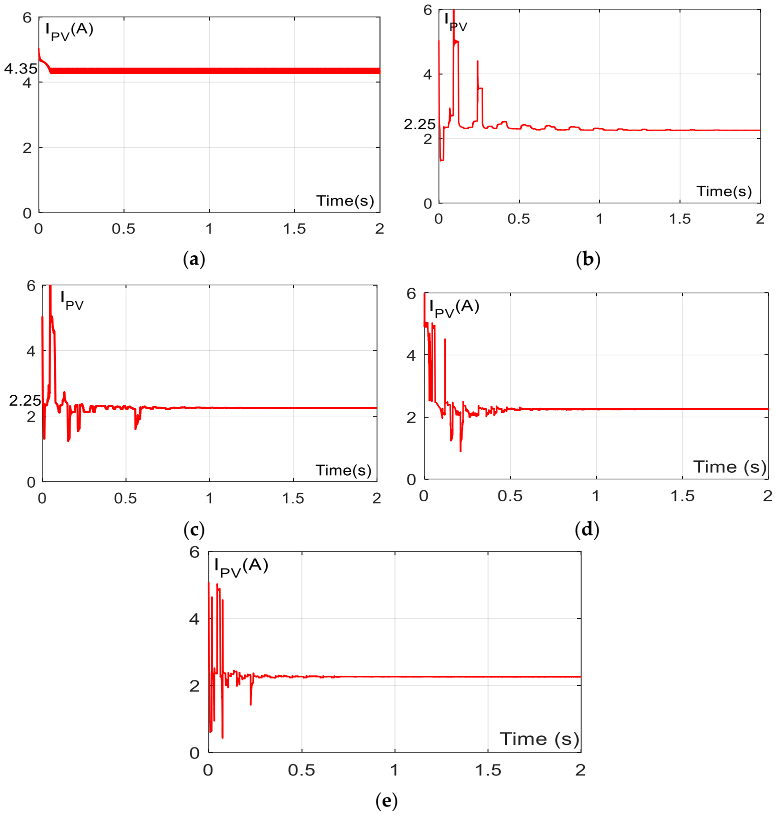

Figure 15. PV current using (**a**) P&O, (**b**) PSO (**c**) CS (**d**) CS-PID and (**e**) CS-STSMC MPPT algorithms.

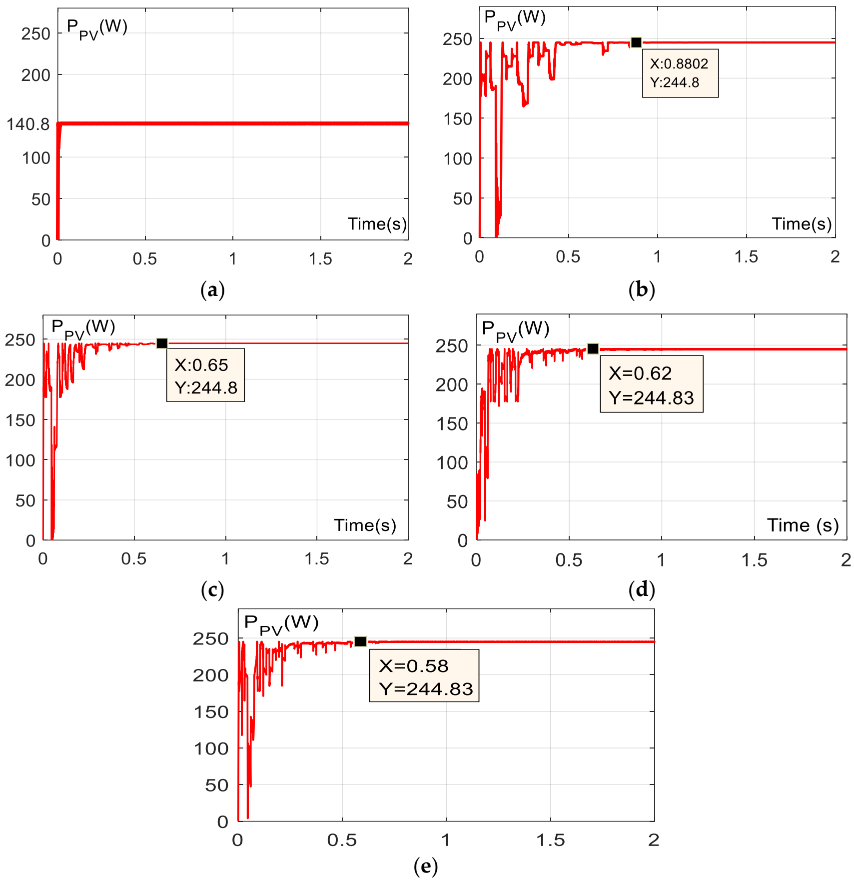

Figure 16. PV power response using (**a**) P&O, (**b**) PSO and (**c**) CS (**d**) CS-PID, and (**e**) CS-STSMC MPPT methods under Case 3.

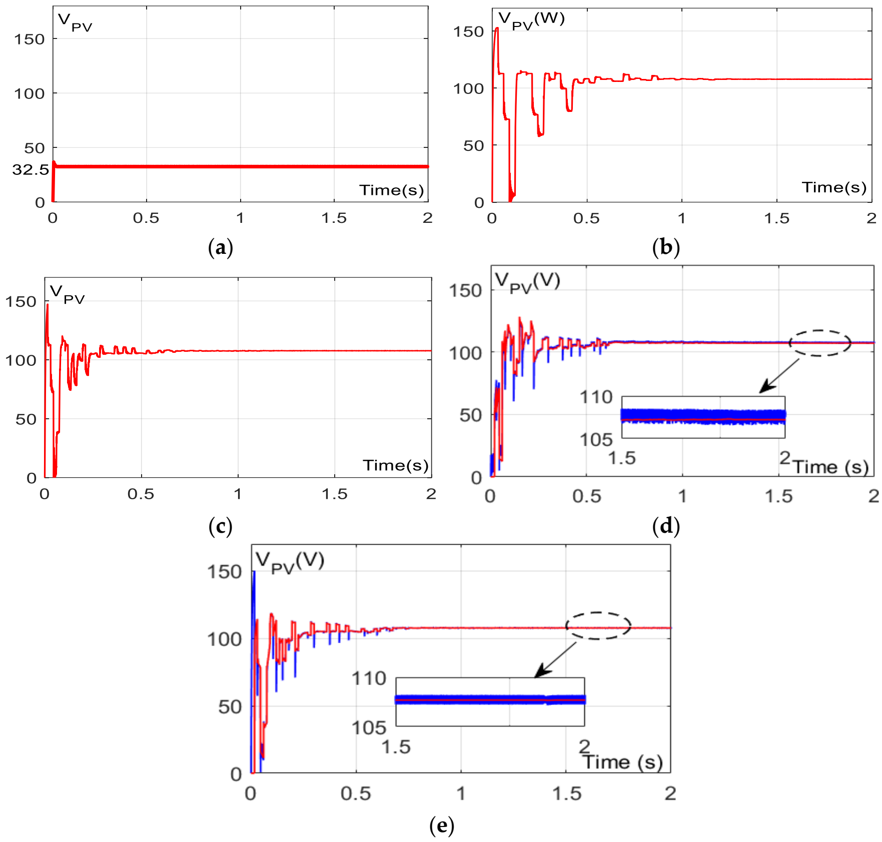

Figure 17. PV voltage using (**a**) P&O, (**b**) PSO, (**c**) CS, (**d**) CS-PID, and (**e**) CS-STSMC MPPT algorithms.

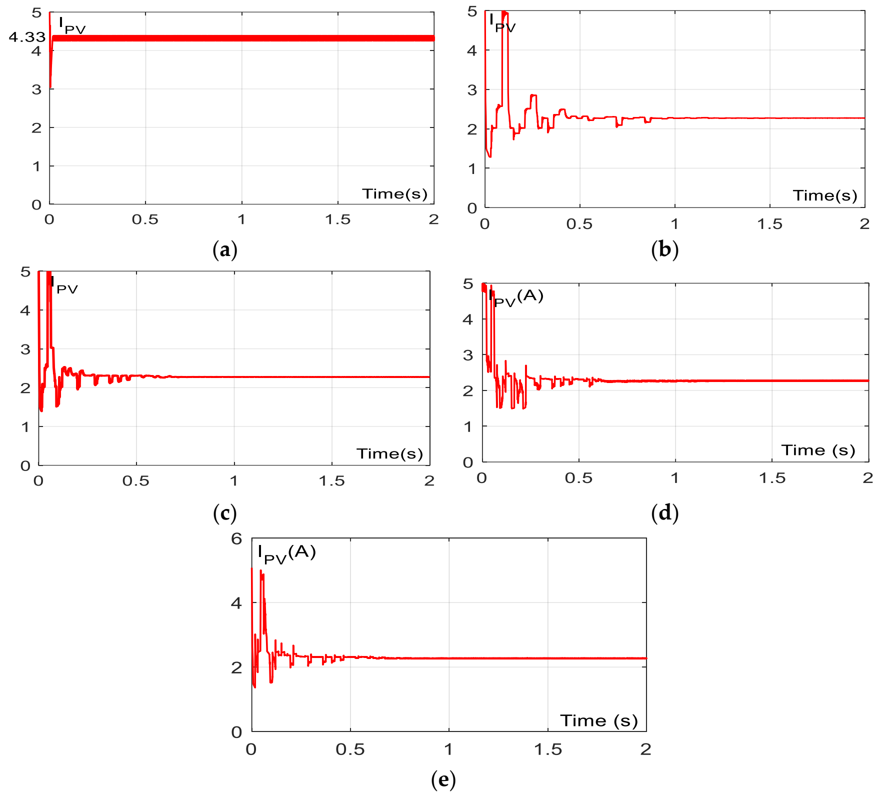

Figure 18. PV current of (**a**) P&O, (**b**) PSO, (**c**) CS, (**d**) CS-PID and (**e**) CS-STSMC MPPT controllers.

6.4. Simulation Comparison

Oscillations, efficiency, power losses, and convergence time are factors used to compare these techniques, which are the CS-STSMC, CS-PID, CS, P&O, and PSO MPPT algorithms under shading cases based on the aforementioned numerical results, as illustrated in Figure 19.

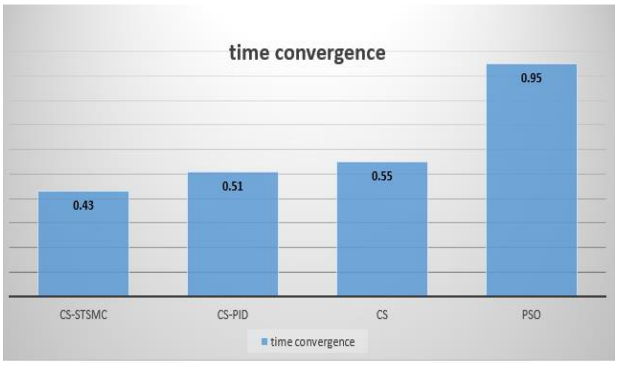

(a)

(b)

Figure 19. Average performance values of CS-STSMC, CS-PID, CS, PSO, and P&O MPPT algorithms in terms of (**a**) convergence time and (**b**) efficiency.

Table 6 resumes the simulation results of the comparison of CS-STSMC with the CS-PID, CS, PSO, and P&O MPPT methods. We notice that the CS-STSMC-MPPT algorithm takes 0.27 s to reach the GMPP in Case 1. Under shading conditions, it only needs 0.43 s in Case 2 and 0.58 s in Case 3. It is noted that the CS-STSMC-MPPT algorithm converges to the GMPP more quickly than the other controllers, while P&O leads to an LMPP under PSCs. According to the performance criteria that are taken into consideration, Figure 19 gives the results obtained and clearly shows that the CS-STSMC-MPPT algorithm is superior to CS-PID, CS, PSO, and P&O.

Table 6. Comparison of the proposed CS-STSMC, CS-PID, CS, PSO, and P&O performance.

Cases	Methods	GMPP	Power Tracked	Power Losses	Convergence Time	Steady State Error	Efficiency
Case 1	Proposed CS-STSMC	600.3	600.3	Very low	0.27 s	neglected	100%
	CS-PID		600.3	high	0.34 s	high	100%
	CS		600.28	Very low	0.42 s	neglected	99.99%
	PSO		600.28	Very low	0.84 s	neglected	99.99%
	P&O		600.1	Medium	0.25 s	high	99.96%
Case 2	Proposed CS-STSMC	326.1	326.1	Low	0.43 s	neglected	100%
	CS-PID		326	high	0.56 s	high	100%
	CS		326.025	low	0.59 s	neglected	99.97%
	PSO		326	low	1.15 s	neglected	99.96%
	P&O		294	9.84%	0.07 s	high	90.15%
Case 3	Proposed CS-STSMC	244.83	244.83	Low	0.58 s	neglected	100%
	CS-PID		244.8	high	0.62 s	high	99.98%
	CS		244.8	low	0.65 s	moderate	99.98%
	PSO		244.8	low	0.88 s	moderate	99.97%
	P&O		140.8	42.5%	0.2 s (LMPP)	high	82.54%

Based on Table 6 and Figure 19, the following points can be mentioned:

- In all PSCs, the GMPP is reached via the CS approach with a very high degree of efficiency. For all of the tested shading cases, 99.98%, 99.97%, and 82.54% are the efficiency average of the CS, PSO, and P&O MPPT algorithms, respectively, as depicted in Figure 19. On the other hand, CS-STSMC and CS-PID achieve 100% of efficiency for different shading scenarios and for any position of the GMPP. Thus, the CS-STSMC and CS-PID MPPT algorithms are more efficient than CS, PSO, and P&O MPPT for any weather condition.
- In the first case, which is zero shading, the CS-STSMC-MPPT algorithm reduces the convergence time by 35.7% and 67.8% compared to conventional CS and PSO, respectively. Compared well to the PID-CS MPPT, CS-STSMC-MPPT minimizes the time of convergence by 20.58% and reaches 21.24% and 6.46% in Case 2 and Case 3 which correspond to weak shading and severe shading, respectively. As a result, the CS-STSMC-MPPT algorithm reduces the convergence time by 16.1% on average in contrast to CS-PID.
- In every case of PSCs, the proposed CS-STSMC-MPPT algorithm always converges to the GMPP. Nevertheless, P&O is tricked into one of the local peaks. For the proposed CS-STSMC-MPPT algorithm, the ripples of the PV voltage decrease which leads to a reduction in the power oscillations, and thus a decrease in the power losses.
- The proposed CS-STSMC-MPPT algorithm reduces the ripples of V_{pv} around the V_{ref} caused by the derivate parameter of PID so, power losses are reduced.

6.5. Qualitative Comparison

An analysis of the seven MPPT methods presented in Table 7 is done to qualitatively compare their performance to that of the proposed CS-STSMC-MPPT algorithm technique under PSCs. These techniques include traditional, soft computing, and hybrid methods.

Table 7. Qualitative comparison between the proposed CS-STSMC-MPPT algorithm and other MPPT methods.

Algorithm	Tracking Efficiency	Oscillations at MPP	Tracking Speed	Hardware Implementation Complexity
INC [131]	Low	High	High	Low
P&O-PSO [132]	Low	High	High	Medium
VSS-P&O [133]	Low	High	Low	Medium
FLC [134]	Low	High	Medium	Medium
GWO [135]	High	Medium	High	Medium
PSO [82]	High	Medium	Low	High
PSO-PI	Medium	high	High	Medium
CSA [15]	High	Low	High	High
Proposed CS-STSMC-MPPT algorithm	Very High	Low	High	Medium

The following factors are used for comparison: the complexity of hardware implementation, oscillations around the MPP, speed of tracking the MPP under PSC, and efficiency in tracking the MPP.

Based on Table 7, we can notice that P&O-PSO, INC, VSS-P&, and FLC are not able to track the GMPP under any shadowing scenario. CSA, PSO, and GWO are metaheuristic methods, and we notice that these algorithms have high tracking efficiency. The CSA MPPT algorithms are fast in tracking the MPP, but the cited traditional methods cannot extract the GMPP in PSCs. Traditional methods, improved P&O, FLC, and PSO-PI generate intense fluctuations close to the MPP in stable conditions, but for the metaheuristic techniques, PSO and GWO oscillations are medium and no steady-state oscillation is seen for CSA and our proposed method. Traditional methods, CSA and CS use few tuning parameters, but the traditional methods and FLC are unable to track the GMPP.

Due to their extremely high efficiency, the metaheuristic methods significantly reduce power losses. Nevertheless, PSO is lower than CSA and PSO-PI in extracting the GMPP. Yet, the proposed CS-STSMC-MPPT algorithm is simpler in hardware implementation than the CSA.

6.6. Quantitative Comparison

Table 8 presents a quantitative comprehensive comparison of nine MPPT algorithms from different categories. We compare the proposed technique with ICS, CSA, VSS-INR, FPA, dynamic group-based cooperation optimization, FLC, and P&O. Each algorithm is assessed based on several key performance parameters. These parameters include the type/nature of the algorithm, its efficiency, and its convergence time under various shading conditions.

Table 8. Quantitative comparison of different MPPT.

Algorithms	MPPT Type	Cases	GMPPT (W)	Efficiency (%)	Convergence Time (ms)	Converter
Proposed CS-STSMC	Metaheuristic	Case1	600.3	100	270	Boost
		Case2	326.1	100	430	
		Case3	244.83	100	580	
Improved CS [16]	Metaheuristic	-	-	99.97	290	Buck boost
CSA [15]	Metaheuristic	Case1 (one peak)	325.5	99.97	310	boost
		Case2 (two peaks)	281.2	99.64	490	
		Case3 (five peaks)	143.2	99.93	360	
Variable step size incremental resistance (VSS-INR) [136]	Metaheuristic	Case1	1339.6	97.82	350	Boost
		Case2	596.8	96.07	391	
		Case3	1407	96.01	501	
PSO & P & O [132]	Hybrid	Case1	239.6	98.41	210	Boost
		Case 2	115.86	98	220	
		Case3	76.57	97.71	298	
Dynamic Group Based Cooperation Optimization [137]	Bio-inspired	-	-	99.88	383	Boost
FLC [136]	AI	Case 1	399.1	99.9	263	Boost
		Case 2	183.0	72.8	255	
		Case 3	95.9	65.5	74	
P & O [15]	Conventional	Case 1 (one peak)	325.5	99.26	650	boost
		Case 2 (two peaks)	281.2	75.32	230	
		Case 3 (five peaks)	143.2	93.57	270	
FPA [18]	Soft computing	Case1 (no shading)	120	99.33	751	boost
		Case2 (weak shading)	55.81	98.98	756	
		Case3 (strong PSC)	42.16	99.74	752	

From this table, we can remark that the metaheuristic methods are particularly effective in PSC, especially the proposed CS-STSMC-MPPT algorithm in terms of efficiency and speed in GMPPT.

To confirm the strength of our algorithm, we cited an example of an improved CS.

7. Conclusions and Futures Works

The proposed CS-STSMC-MPPT algorithm is a combination of the CS-MPPT metaheuristic method and STSMC, which is described in the study as a solution to reduce the negative effects of PSCs on PVS GMPP tracking.

The operation of our proposed CS-STSMC-MPPT algorithm involves two primary parts. The initial part uses the CS-MPPT algorithm to sweep the power-voltage curve to extract the GMPP. Following the identification of the GMPP, the algorithm then generates the corresponding optimal voltage reference. The second part tracks this voltage reference by adjusting the duty cycle of the boost converter. A key attribute of this technique is its efficiency, rapidity in tracking the MPP, reduced power losses, and robustness against variations in parameters.

- The simulation results of this research study have proven the strong capacity of the proposed CS-STSMC-MPPT algorithm to effectively track the GMPP under different shading scenarios, which are zero shading, weak, and severe. The average efficiency of the three tested cases for the CS-STSMC-MPPT approach, which tracks the maximum power from the generator of the PVS, is 100%, compared to other algorithms. Additionally, in PSCs, the total power losses are significantly reduced by the proposed CS-STSMC-MPPT algorithm compared to the CS-PID-MPPT algorithm, because the proposed method decreases the ripples of the PV voltage, which leads to a significant reduction in power losses. In both weak and severe shading scenarios, P&O fails to track the GMPP, and it misleads to an LMPP by an incorrect convergence. Thus, under PSCs, the traditional P&O method fails to detect the GMPP. In contrast, the proposed CS-STSMC-MPPT algorithm reduces the average convergence time in comparison to other MPPT algorithms. CS-STSMC-MPPT reduces the convergence, time by 16.1% on average in contrast to CS-PID with low steady state oscillations while extracting the maximum amount of power hence decreasing power losses. Moreover, a qualitative and quantitative comparison of the proposed CS-STSMC-MPPT algorithm to other methods in the literature demonstrates the superiority of CS-STSMC-MPPT in terms of efficiency, convergence time, and power losses.
- Future research work may be about extending our focus from standalone PVS to grid-connected systems. This broadening of scope will allow us to evaluate our proposed method performance across a wider range of PVS configurations, enhancing its practical relevance Furthermore, the superiority of the proposed CS-STSMC-MPPT algorithm can be validated in an experimental hardware platform.

Author Contributions: Conceptualization, Z.B.H.S., S.K. and B.M.A.; methodology, Z.B.H.S., S.K., M.A.H. and K.A.; software, Z.B.H.S. and S.K.; validation, Z.B.H.S., S.K. and M.A.H.; formal analysis, S.K., M.A.H. and A.A.; investigation, Z.B.H.S., S.K., M.A.H. and A.A.; resources, S.K., M.A.H. and T.G.; data curation, Z.B.H.S., S.K., K.A. and T.G.; writing—original draft preparation, Z.B.H.S., S.K. and T.G.; visualization, Z.B.H.S., S.K., M.A.H. and T.G.; supervision, S.K. and M.A.H.; project administration, B.M.A. and T.G.; funding acquisition, B.M.A. All authors have read and agreed to the published version of the manuscript.

Funding: This research has been funded by the Scientific Research Deanship at the University of Ha'il—Saudi Arabia through project number RG-21 155.

Institutional Review Board Statement: Not applicable.

Informed Consent Statement: Not applicable.

Data Availability Statement: Not applicable.

Conflicts of Interest: The authors declare no conflict of interest.

Nomenclature

PVS	Photovoltaic system
MPP	Maximum power point
MPPT	Maximum power point tracking
GMPPT	Global maximum power point tracking
LMPPT	Local maximum power point tracking
PSC	Partial shading condition
SMC	Sliding Mode Control
STSMC	Super-Twisting Sliding Mode Control
FOSMC	First Order Sliding Mode Control
SOSMC	Second Order Sliding Mode Control
PID	Proportional Integral Derivative
P&O	Perturb and observe
INC	Incremental conductance
HC	Hill climbing
CS	Cuckoo Search
PSO	Particle swarm optimization
AI	Artificial intelligence
ANN	Artificial neural network
FLC	Fuzzy logic control
GA	Genetic algorithm
FPA	Flower pollination algorithm
GWA	Grey wolf algorithm
CSA	Crew search algorithm
PO&GS	Perturb and observe and global scanning
STC	Standard test condition
PWM	Pulse width modulation
P_{best}	Best individual position
G_{besr}	Best swarm position
c_1,c_2	cognitive and social coefficient
ω	weight inertia
α	random step length
λ	parameter that determine the shape of distribution
V_{mpp}	Maximum power point voltage
I_{mpp}	Maximum power point current
V_{mp}, I_{mp}	Maximum photovoltaic system voltage and current
V_o	Open circuit voltage
I_{sc}	Short circuit current

References

1. Ngan, M.S.; Tan, C.W. A study of maximum power point tracking algorithms for stand-alone Photovoltaic Systems. In Proceedings of the 2011 IEEE Applied Power Electronics Colloquium (IAPEC), Johor Bahru, Malaysia, 18–19 April 2011; pp. 22–27. [CrossRef]
2. Singh, S.; Mathew, L. Design and Simulation of Intelligent Control MPPT Technique for PV Module Using. *Int. J. Adv. Res. Electr. Electron. Instrum. Eng.* **2013**, *2*, 4554–4566.
3. Azab, M. A New Maximum Power Point Tracking for Photovoltaic Systems. *Int. J. Electr. Comput. Eng.* **2009**, *3*, 702–705.
4. Motahhir, S.; El Hammoumi, A.; El Ghzizal, A. The most used MPPT algorithms: Review and the suitable low-cost embedded board for each algorithm. *J. Clean. Prod.* **2020**, *246*, 118983. [CrossRef]
5. Li, X.; Wang, Q.; Wen, H.; Xiao, W. Comprehensive Studies on Operational Principles for Maximum Power Point Tracking in Photovoltaic Systems. *IEEE Access* **2019**, *7*, 121407–121420. [CrossRef]
6. Dhimish, M. Assessing MPPT Techniques on Hot-Spotted and Partially Shaded Photovoltaic Modules: Comprehensive Review Based on Experimental Data. *IEEE Trans. Electron. Devices* **2019**, *66*, 1132–1144. [CrossRef]
7. Tafti, H.D.; Sangwongwanich, A.; Yang, Y.; Pou, J.; Konstantinou, G.; Blaabjerg, F. An Adaptive Control Scheme for Flexible Power Point Tracking in Photovoltaic Systems. *IEEE Trans. Power Electron.* **2019**, *34*, 5451–5463. [CrossRef]
8. Syafaruddin; Karatepe, E.; Hiyama, T. Performance enhancement of photovoltaic array through string and central based MPPT system under non-uniform irradiance conditions. *Energy Convers. Manag.* **2012**, *62*, 131–140. [CrossRef]
9. Ghamrawi, A.; Gaubert, J.-P.; Mehdi, D. A new dual-mode maximum power point tracking algorithm based on the Perturb and Observe algorithm used on solar energy system. *Sol. Energy* **2018**, *174*, 508–514. [CrossRef]

10. Abdel-Salam, M.; El-Mohandes, M.-T.; Goda, M. An improved perturb-and-observe based MPPT method for PV systems under varying irradiation levels. *Sol. Energy* **2018**, *171*, 547–561. [CrossRef]
11. Shang, L.; Guo, H.; Zhu, W. An improved MPPT control strategy based on incremental conductance algorithm. *Prot. Control. Mod. Power Syst.* **2020**, *5*, 14. [CrossRef]
12. Eltamaly, A.M.; Abdelaziz, A.Y. (Eds.) *Modern Maximum Power Point Tracking Techniques for Photovoltaic Energy Systems*; Green Energy and Technology; Springer International Publishing: Cham, Switzerland, 2020. [CrossRef]
13. Dirmawan, M.A.; Suhariningsih; Rakhmawati, R. The Comparison Performance of MPPT Perturb and Observe, Fuzzy Logic Controller, and Flower Pollination Algorithm in Normal and Partial Shading Condition. In Proceedings of the 2020 International Electronics Symposium (IES), Surabaya, Indonesia, 29–30 September 2020; pp. 7–13. [CrossRef]
14. Li, G.; Jin, Y.; Akram, M.W.; Chen, X.; Ji, J. Application of bio-inspired algorithms in maximum power point tracking for PV systems under partial shading conditions—A review. *Renew. Sustain. Energy Rev.* **2018**, *81*, 840–873. [CrossRef]
15. Houam, Y.; Terki, A.; Bouarroudj, N. An Efficient Metaheuristic Technique to Control the Maximum Power Point of a Partially Shaded Photovoltaic System Using Crow Search Algorithm (CSA). *J. Electr. Eng. Technol.* **2021**, *16*, 381–402. [CrossRef]
16. Eltamaly, A.M. An Improved Cuckoo Search Algorithm for Maximum Power Point Tracking of Photovoltaic Systems under Partial Shading Conditions. *Energies* **2021**, *14*, 953. [CrossRef]
17. Yu, L.; Zhou, J.; Qin, Z.; Liu, Y.; Zhao, Z.; Bu, L. Artificial Neural Network Training of Unshaded Datasheet for Photovoltaic Maximal Power Point Prediction under Partial Shading Conditions. In Proceedings of the 2022 IEEE 17th Conference on Industrial Electronics and Applications (ICIEA), Chengdu, China, 16–19 December 2022; pp. 1383–1387. [CrossRef]
18. Rezk, H.; AL-Oran, M.; Gomaa, M.R.; Tolba, M.A.; Fathy, A.; Abdelkareem, M.A.; Olabi, A.G.; El-Sayed, A.H.M. A novel statistical performance evaluation of most modern optimization-based global MPPT techniques for partially shaded PV system. *Renew. Sustain. Energy Rev.* **2019**, *115*, 109372. Available online: https://ideas.repec.org//a/eee/rensus/v115y2019ics1364032119305805.html (accessed on 29 May 2023). [CrossRef]
19. Eltamaly, A.M.; Farh, H.M.H.; Al-Saud, M.S. Grade point average assessment for metaheuristic GMPP techniques of partial shaded PV systems. *IET Renew. Power Gener.* **2019**, *13*, 1215–1231. [CrossRef]
20. Bhukya, L.; Kedika, N.R.; Salkuti, S.R. Enhanced Maximum Power Point Techniques for Solar Photovoltaic System under Uniform Insolation and Partial Shading Conditions: A Review. *Algorithms* **2022**, *15*, 365. [CrossRef]
21. What Are the New Implications of Chaos for Unpredictability? Available online: https://www.journals.uchicago.edu/doi/epdf/10.1093/bjps/axn053 (accessed on 10 March 2023).
22. Duan, Q.; Mao, M.; Duan, P.; Hu, B. Application of improved radial basis function neural network method in global MPPT for PV array. In Proceedings of the 2015 IEEE Energy Conversion Congress and Exposition (ECCE), Montreal, QC, Canada, 20–24 September 2015; pp. 3260–3264. [CrossRef]
23. Farhat, S.; Alaoui, R.; Kahaji, A.; Bouhouch, L. Estimating the photovoltaic MPPT by artificial neural network. In Proceedings of the 2013 International Renewable and Sustainable Energy Conference (IRSEC), Ouarzazate, Morocco, 7–9 March 2013; pp. 49–53. [CrossRef]
24. Mahmoud, Y.; Abdelwahed, M.; El-Saadany, E.F. An Enhanced MPPT Method Combining Model-Based and Heuristic Techniques. *IEEE Trans. Sustain. Energy* **2016**, *7*, 576–585. [CrossRef]
25. Yong, Z.; Hong, L.; Liqun, L.; XiaoFeng, G. The MPPT Control Method by Using BP Neural Networks in PV Generating System. In Proceedings of the 2012 International Conference on Industrial Control and Electronics Engineering, Xi'an, China, 23–25 August 2012; pp. 1639–1642. [CrossRef]
26. Chao, K.-H.; Wang, M.-H.; Lee, Y.-H. An extension neural network based incremental MPPT method for a PV system. In Proceedings of the 2011 International Conference on Machine Learning and Cybernetics, Guilin, China, 10–13 July 2011; Volume 2, pp. 654–660. [CrossRef]
27. Ren, Y.; Wang, R.; Rind, S.J.; Zeng, P.; Jiang, L. Speed sensorless nonlinear adaptive control of induction motor using combined speed and perturbation observer. *Control Eng. Pract.* **2022**, *123*, 105166. [CrossRef]
28. Lee, K.; Lee, J.; Lee, Y.I.L. Robust Model Predictive Speed Control of Induction Motors Using a Constrained Disturbance Observer. *Int. J. Control Autom. Syst.* **2020**, *18*, 1539–1549. [CrossRef]
29. Kaced, K.; Larbes, C.; Ait-Chikh, S.M.; Bounabi, M.; Dahmane, Z.E. FPGA implementation of PSO based MPPT for PV systems under partial shading conditions. In Proceedings of the 2017 6th International Conference on Systems and Control (ICSC), Batna, Algeria, 7–9 May 2017; pp. 150–155. [CrossRef]
30. Hadji, S.; Gaubert, J.-P.; Krim, F. Real-Time Genetic Algorithms-Based MPPT: Study and Comparison (Theoretical an Experimental) with Conventional Methods. *Energies* **2018**, *11*, 459. [CrossRef]
31. Rajsekar, N.; Bhardwaj, P.; Pabbewar, A.; Verma, M. Fireworks Algorithm for MPPT. *IJERT* **2016**, *5*, 287–291. [CrossRef]
32. Titri, S.; Larbes, C.; Toumi, K.Y.; Benatchba, K. A new MPPT controller based on the Ant colony optimization algorithm for Photovoltaic systems under partial shading conditions. *Appl. Soft Comput.* **2017**, *58*, 465–479. [CrossRef]
33. El-Helw, H.M.; Magdy, A.; Marei, M.I. A Hybrid Maximum Power Point Tracking Technique for Partially Shaded Photovoltaic Arrays. *IEEE Access* **2017**, *5*, 11900–11908. [CrossRef]
34. Deboucha, H.; Mekhilef, S.; Belaid, S.; Guichi, A. Modified deterministic Jaya (DM-Jaya)-based MPPT algorithm under partially shaded conditions for PV system. *IET Power Electron.* **2020**, *13*, 4625–4632. [CrossRef]

35. Tabrizi, A.; Rahmani, M. Review Some of the Metaheuristic Optimization Algorithms in MPPT. 2021. Available online: https://civilica.com/doc/1031524 (accessed on 1 June 2023).
36. Kennedy, J.; Eberhart, R. Particle Swarm Optimization. In Proceedings of the ICNN'95—International Conference on Neural Networks, Perth, WA, Australia, 27 November–1 December 1995.
37. Mao, M.; Duan, Q.; Duan, P.; Hu, B. Comprehensive improvement of artificial fish swarm algorithm for global MPPT in PV system under partial shading conditions. *Trans. Inst. Meas. Control* **2018**, *40*, 2178–2199. [CrossRef]
38. Abdulaziz, S.; Atlam, G.; Zaki, G.; Nabil, E. Cuckoo search algorithm and particle swarm optimization based maximum power point tracking techniques. *Indones. J. Electr. Eng. Comput. Sci.* **2022**, *26*, 605–616. [CrossRef]
39. Ishaque, K.; Salam, Z.; Amjad, M.; Mekhilef, S. An Improved Particle Swarm Optimization (PSO)–Based MPPT for PV With Reduced Steady-State Oscillation. *IEEE Trans. Power Electron.* **2012**, *27*, 3627–3638. [CrossRef]
40. Ahmed, J.; Salam, Z. A Maximum Power Point Tracking (MPPT) for PV system using Cuckoo Search with partial shading capability. *Appl. Energy* **2014**, *119*, 118–130. [CrossRef]
41. Ahmed, J.; Salam, Z. A soft computing MPPT for PV system based on Cuckoo Search algorithm. In Proceedings of the 4th International Conference on Power Engineering, Energy and Electrical Drives, Istanbul, Turkey, 13–17 May 2013; pp. 558–562. [CrossRef]
42. Al-Wesabi, I.; Fang, Z.; Farh, H.M.H.; Al-Shamma'a, A.A.; Al-Shaalan, A.M.; Kandil, T.; Ding, M. Cuckoo Search Combined with PID Controller for Maximum Power Extraction of Partially Shaded Photovoltaic System. *Energies* **2022**, *15*, 2513. [CrossRef]
43. Ali, E.M.; Abdelsalam, A.K.; Youssef, K.H.; Hossam-Eldin, A.A. An Enhanced Cuckoo Search Algorithm Fitting for Photovoltaic Systems' Global Maximum Power Point Tracking under Partial Shading Conditions. *Energies* **2021**, *14*, 7210. [CrossRef]
44. Mosaad, M.I.; abed el-Raouf, M.O.; Al-Ahmar, M.A.; Banakher, F.A. Maximum Power Point Tracking of PV system Based Cuckoo Search Algorithm; review and comparison. *Energy Procedia* **2019**, *162*, 117–126. [CrossRef]
45. Baset, A.; Halim, A.; Saad, N.; El-Sattar, A. A Comparative Study Between Perturb and Observe and Cuckoo Search Algorithm for Maximum Power Point Tracking. In Proceedings of the 2019 21st International Middle East Power Systems Conference (MEPCON), Cairo, Egypt, 17–19 December 2019; p. 723. [CrossRef]
46. Spertino, F.; Akilimali, J.S. Are Manufacturing I–V Mismatch and Reverse Currents Key Factors in Large Photovoltaic Arrays? *IEEE Trans. Ind. Electron.* **2009**, *56*, 4520–4531. [CrossRef]
47. Kang, T.; Yao, J.; Jin, M.; Yang, S.; Duong, T. A Novel Improved Cuckoo Search Algorithm for Parameter Estimation of Photovoltaic (PV) Models. *Energies* **2018**, *11*, 1060. [CrossRef]
48. Chao, K.-H.; Chang, L.-Y.; Wang, K.-W. Global Maximum Power Point Tracking of Photovoltaic Module Arrays Based on Improved Cuckoo Search Algorithm. *Electronics* **2022**, *11*, 1247. [CrossRef]
49. Mohammedi, A.; Benslimane, T. Development of rapid and reliable cuckoo search algorithm for global maximum power point tracking of solar PV systems in partial shading condition. *Arch. Control. Sci.* **2021**, *31*, 495–526. [CrossRef]
50. Liu, X.; Yu, H.; Yu, J.; Zhao, L. Combined Speed and Current Terminal Sliding Mode Control with Nonlinear Disturbance Observer for PMSM Drive. *IEEE Access* **2018**, *6*, 29594–29601. [CrossRef]
51. Krim, S.; Gdaim, S.; Mtibaa, A.; Mimouni, M.F. Implementation on the FPGA of DTC-SVM Based Proportional Integral and Sliding Mode Controllers of an Induction Motor: A Comparative Study. *J. Circuits Syst. Comput.* **2017**, *26*, 1750049. Available online: https://www.worldscientific.com/doi/10.1142/S0218126617500499 (accessed on 1 June 2023). [CrossRef]
52. Yilmaz, U.; Kircay, A.; Borekci, S. PV system fuzzy logic MPPT method and PI control as a charge controller. *Renew. Sustain. Energy Rev.* **2018**, *81*, 994–1001. [CrossRef]
53. Touil, S.-A.; Boudjerda, N.; Boubakir, A.; El Khamlichi Drissi, K. A sliding mode control and artificial neural network based MPPT for a direct grid-connected photovoltaic source. *Asian J. Control.* **2019**, *21*, 1892–1905. [CrossRef]
54. Chaibi, Y.; Salhi, M.; El-jouni, A. Sliding Mode Controllers for Standalone PV Systems: Modeling and Approach of Control. *Int. J. Photoenergy* **2019**, *2019*, e5092078. [CrossRef]
55. Ali, N.; Armghan, H.; Ahmad, I.; Armghan, A.; Khan, S.; Arsalan, M. Backstepping based non-linear control for maximum power point tracking in photovoltaic system. *Sol. Energy* **2018**, *159*, 134–141. [CrossRef]
56. Ahmed, S.; Muhammad Adil, H.M.; Ahmad, I.; Azeem, M.K.; e Huma, Z.; Abbas Khan, S. Supertwisting Sliding Mode Algorithm Based Nonlinear MPPT Control for a Solar PV System with Artificial Neural Networks Based Reference Generation. *Energies* **2020**, *13*, 3695. [CrossRef]
57. Rafiq, M.; Rehman, S.; Rehman, F.; Butt, Q.R.; Awan, I. A second order sliding mode control design of a switched reluctance motor using super twisting algorithm. *Simul. Model. Pract. Theory* **2012**, *25*, 106–117. [CrossRef]
58. Zou, Q. Adaptive Sliding Mode Control for Chain Driving System with Disturbance Observer. *Proc. Inst. Mech. Eng. Part I J. Syst. Control Eng.* **2020**, *234*, 1050–1059. Available online: https://journals.sagepub.com/doi/abs/10.1177/0959651819895693?journalCode=piia (accessed on 1 June 2023). [CrossRef]
59. Gohar Ali, H.; Arbos, R.V. Chattering Free Adaptive Sliding Mode Controller for Photovoltaic Panels with Maximum Power Point Tracking. *Energies* **2020**, *13*, 5678. [CrossRef]
60. Kihal, A.; Krim, F.; Laib, A.; Talbi, B.; Afghoul, H. An improved MPPT scheme employing adaptive integral derivative sliding mode control for photovoltaic systems under fast irradiation changes. *ISA Trans.* **2019**, *87*, 297–306. [CrossRef]

61. Xu, R.; Zhou, M. Sliding mode control with sigmoid function for the motion tracking control of the piezo-actuated stages. *Electron. Lett.* **2017**, *53*, 75–77. Available online: https://ietresearch.onlinelibrary.wiley.com/doi/10.1049/el.2016.3558 (accessed on 1 June 2023). [CrossRef]
62. Krim, S.; Gdaim, S.; Abdellatif, M.; Mimouni, M. Real time implementation of DTC based on Sliding Mode Speed Controller of an Induction Motor. In Proceedings of the 2015 16th International Conference on Sciences and Techniques of Automatic Control and Computer Engineering (STA), Monastir, Tunisia, 21–23 December 2015. [CrossRef]
63. Mishra, R.; Mohanty, K. Development and implementation of induction motor drive using sliding-mode based simplified neuro-fuzzy control. *Eng. Appl. Artif. Intell.* **2020**, *91*, 103593. [CrossRef]
64. Bakkar, M.; Aboelhassan, A.; Abdelgeliel, M.; Galea, M. PV Systems Control Using Fuzzy Logic Controller Employing Dynamic Safety Margin under Normal and Partial Shading Conditions. *Energies* **2021**, *14*, 841. [CrossRef]
65. Ahmad, F.F.; Ghenai, C.; Hamid, A.K.; Bettayeb, M. Application of sliding mode control for maximum power point tracking of solar photovoltaic systems: A comprehensive review. *Annu. Rev. Control* **2020**, *49*, 173–196. [CrossRef]
66. Gambhire, S.J.; Kishore, D.R.; Londhe, P.S.; Pawar, S.N. Review of sliding mode based control techniques for control system applications. *Int. J. Dynam. Control* **2021**, *9*, 363–378. [CrossRef]
67. Second-Order Sliding-Mode Control—An Overview | ScienceDirect Topics. Available online: https://www.sciencedirect.com/topics/engineering/second-order-sliding-mode-control (accessed on 1 June 2023).
68. Krim, S.; Mimouni, M.F. Design and Xilinx Virtex-field-programmable gate array for hardware in the loop of sensorless second-order sliding mode control and model reference adaptive system–sliding mode observer for direct torque control of induction motor drive. *Proc. Inst. Mech. Eng. Part I J. Syst. Control Eng.* **2023**, *237*, 839–869. [CrossRef]
69. Mao, M.; Cui, L.; Zhang, Q.; Guo, K.; Zhou, L.; Huang, H. Classification and summarization of solar photovoltaic MPPT techniques: A review based on traditional and intelligent control strategies. *Energy Rep.* **2020**, *6*, 1312–1327. [CrossRef]
70. Hanzaei, S.H.; Gorji, S.A.; Ektesabi, M. A Scheme-Based Review of MPPT Techniques with Respect to Input Variables Including Solar Irradiance and PV Arrays' Temperature. *IEEE Access* **2020**, *8*, 182229–182239. [CrossRef]
71. Karami, N.; Moubayed, N.; Outbib, R. General review and classification of different MPPT Techniques. *Renew. Sustain. Energy Rev.* **2017**, *68*, 1–18. [CrossRef]
72. Podder, A.K.; Roy, N.K.; Pota, H.R. MPPT methods for solar PV systems: A critical review based on tracking nature. *IET Renew. Power Gener.* **2019**, *13*, 1615–1632. [CrossRef]
73. Ram, J.P.; Babu, T.S.; Rajasekar, N. A comprehensive review on solar PV maximum power point tracking techniques. *Renew. Sustain. Energy Rev.* **2017**, *67*, 826–847. [CrossRef]
74. Hashim, N.; Salam, Z. Critical evaluation of soft computing methods for maximum power point tracking algorithms of photovoltaic systems. *Int. J. Power Electron. Drive Syst.* **2019**, *10*, 548. [CrossRef]
75. Bendib, B.; Belmili, H.; Krim, F. A survey of the most used MPPT methods: Conventional and advanced algorithms applied for photovoltaic systems. *Renew. Sustain. Energy Rev.* **2015**, *45*, 637–648. [CrossRef]
76. Balamurugan, M.; Sahoo, S.K.; Sukchai, S. Application of soft computing methods for grid connected PV system: A technological and status review. *Renew. Sustain. Energy Rev.* **2017**, *75*, 1493–1508. [CrossRef]
77. Bollipo, R.B.; Mikkili, S.; Bonthagorla, P.K. Hybrid, optimal, intelligent and classical PV MPPT techniques: A review. *CSEE J. Power Energy Syst.* **2021**, *7*, 9–33. [CrossRef]
78. Premkumar, M.; Sowmya, R. Certain Study on MPPT Algorithms to track the Global MPP under Partial Shading on Solar PV Module/Array. *Int. J. Comput. Digit. Syst.* **2019**, *8*, 405–416. [CrossRef]
79. Reza Reisi, A.; Hassan Moradi, M.; Jamasb, S. Classification and comparison of maximum power point tracking techniques for photovoltaic system: A review. *Renew. Sustain. Energy Rev.* **2013**, *19*, 433–443. [CrossRef]
80. Mellit, A.; Kalogirou, S.A. Artificial intelligence techniques for photovoltaic applications: A review. *Prog. Energy Combust. Sci.* **2008**, *34*, 574–632. [CrossRef]
81. Ivancevic, V.G.; Ivancevic, T.T. *Complex Nonlinearity: Chaos, Phase Transitions, Topology Change and Path*; Springer: Berlin/Heidelberg, Germany, 2008.
82. Rezk, H.; Fathy, A.; Abdelaziz, A.Y. A comparison of different global MPPT techniques based on meta-heuristic algorithms for photovoltaic system subjected to partial shading conditions. *Renew. Sustain. Energy Rev.* **2017**, *74*, 377–386. [CrossRef]
83. Bataineh, K. Improved hybrid algorithms-based MPPT algorithm for PV system operating under severe weather conditions. *IET Power Electron.* **2019**, *12*, 703–711. [CrossRef]
84. Lyden, S.; Haque, M.E. Maximum Power Point Tracking techniques for photovoltaic systems: A comprehensive review and comparative analysis. *Renew. Sustain. Energy Rev.* **2015**, *52*, 1504–1518. [CrossRef]
85. Ramli, M.A.M.; Twaha, S.; Ishaque, K.; Al-Turki, Y.A. A review on maximum power point tracking for photovoltaic systems with and without shading conditions. *Renew. Sustain. Energy Rev.* **2017**, *67*, 144–159. [CrossRef]
86. Belhachat, F.; Larbes, C. A review of global maximum power point tracking techniques of photovoltaic system under partial shading conditions. *Renew. Sustain. Energy Rev.* **2018**, *92*, 513–553. [CrossRef]
87. Singh, B.; Sharma, U.; Kumar, S. Standalone Photovoltaic Water Pumping System Using Induction Motor Drive with Reduced Sensors. *IEEE Trans. Ind. Appl.* **2018**, *54*, 3645–3655. [CrossRef]

88. Hiyama, T.; Karatepe, E. Investigation of ANN performance for tracking the optimum points of PV module under partially shaded conditions. In Proceedings of the 2010 Conference Proceedings IPEC, Singapore, 27–29 October 2010; Available online: https://ieeexplore.ieee.org/document/5697002 (accessed on 11 June 2022).
89. Yadav, A.; Pachauri, R.; Chauhan, Y. Comprehensive investigation of PV arrays with puzzle shade dispersion for improved performance. *Sol. Energy* **2016**, *129*, 256–285. [CrossRef]
90. Javed, K.; Ashfaq, H.; Singh, R. A new simple MPPT algorithm to track MPP under partial shading for solar photovoltaic systems. *Int. J. Green Energy* **2020**, *17*, 48–61. Available online: https://www.tandfonline.com/doi/abs/10.1080/15435075.2019.1686001 (accessed on 18 September 2022). [CrossRef]
91. Xiao, W.; Dunford, W.G. A modified adaptive hill climbing MPPT method for photovoltaic power systems. In Proceedings of the 2004 IEEE 35th Annual Power Electronics Specialists Conference (IEEE Cat. No.04CH37551), Aachen, Germany, 20–25 June 2004; Volume 3, pp. 1957–1963. [CrossRef]
92. Veerapen, S.; Wen, H.; Du, Y. Design of a novel MPPT algorithm based on the two stage searching method for PV systems under partial shading. In Proceedings of the 2017 IEEE 3rd International Future Energy Electronics Conference and ECCE Asia (IFEEC 2017—ECCE Asia), Kaohsiung, Taiwan, 3–7 June 2017; pp. 1494–1498. [CrossRef]
93. Ali, A.I.M.; Mohamed, H.R.A. Improved P&O MPPT algorithm with efficient open-circuit voltage estimation for two-stage grid-integrated PV system under realistic solar radiation. *Int. J. Electr. Power Energy Syst.* **2022**, *137*, 107805. [CrossRef]
94. Sher, H.A.; Rizvi, A.A.; Addoweesh, K.E.; Al-Haddad, K. A Single-Stage Stand-Alone Photovoltaic Energy System with High Tracking Efficiency. *IEEE Trans. Sustain. Energy* **2017**, *8*, 755–762. [CrossRef]
95. Udavalakshmi, J.K.; Sheik, M.S. Comparative Study of Perturb & Observe and Look-Up Table Maximum Power Point Tracking Techniques using MATLABISimulink. In Proceedings of the 2018 International Conference on Current Trends towards Converging Technologies (ICCTCT), Coimbatore, India, 1–3 March 2018; pp. 1–5. [CrossRef]
96. Hadji, S.; Gaubert, J.-P.; Krim, F. Maximum Power Point Tracking (MPPT) for Photovoltaic systems using open circuit voltage and short circuit current. In Proceedings of the 3rd International Conference on Systems and Control, Algiers, Algeria, 29–31 October 2013; pp. 87–92. [CrossRef]
97. Li, M.; Huang, X.; Liu, H.; Liu, B.; Wu, Y.; Xiong, A.; Dong, T. Prediction of gas solubility in polymers by back propagation artificial neural network based on self-adaptive particle swarm optimization algorithm and chaos theory. *Fluid Phase Equilibria* **2013**, *356*, 11–17. [CrossRef]
98. Nehmzow, U.; Walker, K. Quantitative description of robot–environment interaction using chaos theory. *Robot. Auton. Syst.* **2005**, *53*, 177–193. [CrossRef]
99. Safonov, L.A.; Tomer, E.; Strygin, V.V.; Ashkenazy, Y.; Havlin, S. Multifractal chaotic attractors in a system of delay-differential equations modeling road traffic: Chaos: An Interdisciplinary. *J. Nonlinear Sci.* **2002**, *12*, 1006–1014. Available online: https://aip.scitation.org/doi/abs/10.1063/1.1507903 (accessed on 10 March 2023). [CrossRef] [PubMed]
100. Zhou, L.; Chen, Y.; Guo, K.; Jia, F. New Approach for MPPT Control of Photovoltaic System with Mutative-Scale Dual-Carrier Chaotic Search. *IEEE Trans. Power Electron.* **2011**, *26*, 1038–1048. [CrossRef]
101. Bouselham, L.; Hajji, M.; Hajji, B.; Bouali, H. A New MPPT-based ANN for Photovoltaic System under Partial Shading Conditions. *Energy Procedia* **2017**, *111*, 924–933. Available online: https://reader.elsevier.com/reader/sd/pii/S1876610217302886?token=65E1FD0FED63F608C1A5E026FF9295BAC31D8BDE1369FDE56BE3EC49F7B3E9C06AA6A4FB2F3762E5E26C9BCD5B748711&originRegion=eu-west-1&originCreation=20230125131607 (accessed on 25 January 2023). [CrossRef]
102. Chekired, F.; Larbes, C.; Rekioua, D.; Haddad, F. Implementation of a MPPT fuzzy controller for photovoltaic systems on FPGA circuit. *Energy Procedia* **2011**, *6*, 541–549. [CrossRef]
103. Seyedmahmoudian, M.; Horan, B.; Soon, T.K.; Rahmani, R.; Than Oo, A.M.; Mekhilef, S.; Stojcevski, A. State of the art artificial intelligence-based MPPT techniques for mitigating partial shading effects on PV systems—A review. *Renew. Sustain. Energy Rev.* **2016**, *64*, 435–455. [CrossRef]
104. Tey, K.S.; Mekhilef, S.; Seyedmahmoudian, M.; Horan, B.; Oo, A.T.; Stojcevski, A. Improved Differential Evolution-Based MPPT Algorithm Using SEPIC for PV Systems Under Partial Shading Conditions and Load Variation. *IEEE Trans. Ind. Inform.* **2018**, *14*, 4322–4333. [CrossRef]
105. Lodhi, E.; Shafqat, R.N.; Kerrouche, K.D.E.; Lodhi, Z. Application of Particle Swarm Optimization for Extracting Global Maximum Power Point in PV System under Partial Shadow Conditions. *IJEEE* **2017**, *5*, 223–229. [CrossRef]
106. Huang, C.; Wang, L.; Yeung, R.S.-C.; Zhang, Z.; Chung, H.S.-H.; Bensoussan, A. A Prediction Model-Guided Jaya Algorithm for the PV System Maximum Power Point Tracking. *IEEE Trans. Sustain. Energy* **2018**, *9*, 45–55. [CrossRef]
107. Cherukuri, S.K.; Rayapudi, S. Enhanced Grey Wolf Optimizer based MPPT Algorithm of PV system under Partial Shaded Condition. *Int. J. Renew. Energy Dev.* **2017**, *6*, 203. [CrossRef]
108. Sawant, P.T.; Lbhattar, P.C.; Bhattar, C.L. Enhancement of PV system based on artificial bee colony algorithm under dynamic conditions. In Proceedings of the 2016 IEEE International Conference on Recent Trends in Electronics, Information & Communication Technology (RTEICT), Bangalore, India, 20–21 May 2016; pp. 1251–1255. [CrossRef]
109. Chang, W.K.; Lin, C.K.; Chuan, D.C.; Chao, Y.C. Chang Duodenogastric reflux: Proposed new endoscopic classification in symptomatic patients. *J. Med. Sci.* **2016**, *36*, 1–5. Available online: https://www.jmedscindmc.com/article.asp?issn=1011-4564;year=2016;volume=36;issue=1;spage=1;epage=5;aulast=Chang (accessed on 4 June 2022).

110. Rezk, H.; Fathy, A. Simulation of global MPPT based on teaching–learning-based optimization technique for partially shaded PV system. *Electr. Eng.* **2017**, *99*, 847–859. [CrossRef]
111. Mohanty, S.; Subudhi, B.; Ray, P.K. A Grey Wolf-Assisted Perturb & Observe MPPT Algorithm for a PV System. *IEEE Trans. Energy Convers.* **2017**, *32*, 340–347. [CrossRef]
112. Manickam, C.; Raman, G.P.; Raman, G.R.; Ganesan, S.I.; Chilakapati, N. Fireworks Enriched P&O Algorithm for GMPPT and Detection of Partial Shading in PV Systems. *IEEE Trans. Power Electron.* **2017**, *32*, 4432–4443. [CrossRef]
113. Yang, Z.; Duan, Q.; Zhong, J.; Mao, M.; Xun, Z. Analysis of improved PSO and perturb & observe global MPPT algorithm for PV array under partial shading condition. In Proceedings of the 2017 29th Chinese Control and Decision Conference (CCDC), Chongqing, China, 28–30 May 2017; pp. 549–553. [CrossRef]
114. Shi, J.; Wang, Z.; Wang, X. Innovations in the sustainable management of local government liabilities in China. *Singap. Econ. Rev.* **2018**, *63*, 819–837. [CrossRef]
115. DemiRel, H.; Karagöz, M.K.; Erkal, B. A Novel MPPT Method for PV Arrays Based on Modified Bat Algorithm and Incremental Conductance Algorithm with Partial Shading Capability. In Proceedings of the First International Conference on Energy Systems Engineering, Karabuk, Turkey, 2–4 November 2017; Volume 6.
116. Nayak, B.K.; Mohapatra, A.; Mohanty, K.B. Parameters estimation of photovoltaic module using nonlinear least square algorithm: A comparative study. In Proceedings of the 2013 Annual IEEE India Conference (INDICON), Mumbai, India, 13–15 December 2013; pp. 1–6. [CrossRef]
117. Nayak, B.; Mohapatra, A.; Mohanty, K.B. Selection criteria of dc-dc converter and control variable for MPPT of PV system utilized in heating and cooking applications. *Cogent Eng.* **2017**, *4*, 1363357. [CrossRef]
118. Khan, M.Z.; Khan, Z.; Khan, M.N.I.; Saha, S.; Noor, D.F.; Rachi, M.R.K. Maximum Power Point Tracking for Photovoltaic Array Using Parabolic Interpolation. *Int. J. Inf. Electron. Eng.* **2014**, *4*, 249–255. [CrossRef]
119. Xuesong, Z.; Daichun, S.; Youjie, M.; Deshu, C. The simulation and design for MPPT of PV system Based on Incremental Conductance Method. In Proceedings of the 2010 WASE International Conference on Information Engineering, BeiDai, China, 14–15 August 2010; Volume 2, pp. 314–317. [CrossRef]
120. Van Dijk, E.; Spruijt, J.N.; O'Sullivan, D.M.; Klaassens, J.B. PWM-switch modeling of DC-DC converters. *IEEE Trans. Power Electron.* **1995**, *10*, 659–665. [CrossRef]
121. Motahhir, S.; Eltamaly, A. *Advanced Technologies for Solar Photovoltaics Energy Systems*; Springer: Berlin/Heidelberg, Germany, 2021. [CrossRef]
122. Kuvshinov, V.V.; Abd Ali, L.M.; Kakushina, E.G.; Krit, B.L.; Morozova, N.V.; Kuvshinova, V.V. Studies of the PV Array Characteristics with Changing Array Surface Irradiance. *Appl. Sol. Energy* **2019**, *55*, 223–228. Available online: https://link.springer.com/article/10.3103/S0003701X19040054 (accessed on 18 September 2022). [CrossRef]
123. Abdel-Salam, M.; El-Mohandes, M.; El-Ghazaly, M. An Efficient Tracking of MPP in PV Systems Using a Newly-Formulated P&O-MPPT Method Under Varying Irradiation Levels. *J. Electr. Eng. Technol.* **2019**, *15*, 501–513. [CrossRef]
124. Saidi, K.; Maamoun, M.; Bounekhla, M. A new high performance variable step size perturb-and-observe MPPT algorithm for photovoltaic system. *Int. J. Power Electron. Drive Syst.* **2019**, *10*, 1662. [CrossRef]
125. Harrag, A.; Messalti, S. Variable step size modified P&O MPPT algorithm using GA-based hybrid offline/online PID controller. *Renew. Sustain. Energy Rev.* **2015**, *49*, 1247–1260. [CrossRef]
126. Khan, S.U.; Yang, S.; Wang, L.; Liu, L. A Modified Particle Swarm Optimization Algorithm for Global Optimizations of Inverse Problems. *IEEE Trans. Magn.* **2016**, *52*, 1–4. [CrossRef]
127. Rajabioun, R. Cuckoo Optimization Algorithm. *Appl. Soft Comput.* **2011**, *11*, 5508–5518. [CrossRef]
128. Utkin, V.I. Sliding mode control design principles and applications to electric drives. *IEEE Trans. Ind. Electron.* **1993**, *40*, 23–36. [CrossRef]
129. Amet, L.; Ghanes, M.; Barbot, J.-P. HOSM control under quantization and saturation constraints: Zig-Zag design solutions. In Proceedings of the 2012 IEEE 51st IEEE Conference on Decision and Control (CDC), Maui, HI, USA, 10–13 December 2012; pp. 5494–5498. [CrossRef]
130. Souissi, A. Adaptive sliding mode control of a PEM fuel cell system based on the super twisting algorithm. *Energy Rep.* **2021**, *7*, 3390–3399. [CrossRef]
131. Motahhir, S.; El Hammoumi, A.; El Ghzizal, A. Photovoltaic system with quantitative comparative between an improved MPPT and existing INC and P&O methods under fast varying of solar irradiation. *Energy Rep.* **2018**, *4*, 341–350. [CrossRef]
132. Hanafiah, S.; Ayad, A.; Hehn, A.; Kennel, R. A hybrid MPPT for quasi-Z-source inverters in PV applications under partial shading condition. In Proceedings of the 2017 11th IEEE International Conference on Compatibility, Power Electronics and Power Engineering (CPE-POWERENG), Cadiz, Spain, 4–6 April 2017; pp. 418–423. [CrossRef]
133. Sarika, P.E.; Jacob, J.; Mohammed Sulthan, S.; Paul, S. A Novel Hybrid Maximum Power Point Tracking Technique with Zero Oscillation Based on P&O Algorithm. *Int. J. Renew. Energy Res.* **2020**, *10*, 1962–1973.
134. Kandemir, E.; Cetin, N.S.; Borekci, S. Single-stage photovoltaic system design based on energy recovery and fuzzy logic control for partial shading condition. *Int. J. Circuit Theory Appl.* **2022**, *50*, 1770–1792. Available online: https://onlinelibrary.wiley.com/doi/full/10.1002/cta.3223 (accessed on 8 November 2022). [CrossRef]
135. Eltamaly, A.; Hussein Farh, H.M. Dynamic global maximum power point tracking of the PV systems under variant partial shading using hybrid GWO-FLC. *Sol. Energy* **2019**, *177*, 306–316. [CrossRef]

136. Nemours, J.A.; Chowdhury, S. Performance Analysis of Fuzzy Logic Maximum Power Point Tracking Scheme for Solar PV System Under Varying Load and Atmospheric Conditions. In Proceedings of the 2019 IEEE PES/IAS PowerAfrica, Abuja, Nigeria, 20–23 August 2019; pp. 134–139. [CrossRef]
137. Moosavi, S.K.R.; Mansoor, M.; Zafar, M.H.; Khan, N.M.; Mirza, A.F.; Akhtar, N. Highly efficient maximum power point tracking control technique for PV system under dynamic operating conditions. *Energy Rep.* **2022**, *8*, 13529–13543. [CrossRef]

Disclaimer/Publisher's Note: The statements, opinions and data contained in all publications are solely those of the individual author(s) and contributor(s) and not of MDPI and/or the editor(s). MDPI and/or the editor(s) disclaim responsibility for any injury to people or property resulting from any ideas, methods, instructions or products referred to in the content.